Using ^{81}Kr and isotopic tracers to characterize old groundwater in the Bangkok metropolitan and vicinity areas

Kiattipong Kamdee[1], Jose A. Corcho Alvarado[2,*], Monthon Yongprawat[1], Occapasorn Occarach[3], Vanachawan Hunyek[3], Arpakorn Wongsit[3], Chakrit Saengkorakot[1], Patchareeya Chanruang[1], Chalermpong Polee[1], Nichtima Uapoonphol[1], Jennifer Mabry[4], Nicolo Romeo[4], Darren Hillegonds[4(#)], Jake C. Zappala[5], Peter Mueller[5], Takuya Matsumoto[4]

[1] *Thailand Institute of Nuclear Technology (Public Organization), Nakhon Nayok, Thailand*

[2] *Nuclear Chemistry Division, Spiez Laboratory, Federal Office for Civil Protection, CH-3700 Spiez, Switzerland*

[3] *Department of Groundwater Resources, Ministry of Natural Resources and Environment, Bangkok, Thailand*

[4] *Isotope Hydrology Laboratory, Division of Physical and Chemical Sciences, Department of Nuclear Sciences and Applications, International Atomic Energy Agency*

[5] *Physics Division, Argonne National Laboratory, Lemont, IL 60439, USA*

(# Present address: Noble Gas Mass Spectrometry Laboratory, University of Oxford, Department of Earth Sciences, UK)

*Corresponding author: Dr. José A. Corcho Alvarado, jose.corcho@babs.admin.ch

Using ^{81}Kr and isotopic tracers to characterize old groundwater in the Bangkok metropolitan and vicinity areas

Krypton-81 was applied to investigate the age of groundwater in the aquifer system in the Bangkok metropolitan and vicinity areas. Stable (^{2}H, ^{18}O and ^{13}C) and radioactive (^{3}H, ^{85}Kr and ^{14}C) isotopes and noble gases were applied in parallel. ^{14}C varied from 66 pMC in the upper aquifers, to near the limit of detection in the deeper aquifers. Low levels of ^{14}C and significant radiogenic ^{4}He confirm that groundwater in the deep aquifers is older than 30 ka. ^{81}Kr analysis identified groundwater with ages ranging from 17 to 300 ka. At some sites, large age discrepancies between ^{81}Kr and ^{14}C indicated that inter-aquifer mixing is likely occurring. Stable noble gas concentrations suggest that groundwaters in the deeper aquifers, with apparent ages of 300 to 10 ka, have recharged in slightly colder and wetter climates than those found in the upper aquifers with apparent ages < 10 ka. Degradation of the water quality from past seawater intrusion was identified in the upper four aquifers. This was also evidenced by enriched δ^{18}O and δ^{2}H values, which are typical of seawater. The four deeper aquifers contain high quality water characterized by less enriched δ^{18}O and δ^{2}H values. This work presents new findings of very old groundwater in the Bangkok aquifer system. As deep aquifers contain good quality water that is very old and non-renewable on human timescales, their exploitation needs to be carefully planned in order to maintain a sustainable supply of fresh water.

Keywords: Thailand, groundwater age, ^{81}Kr, ^{14}C, noble gases

Introduction

The Lower Chao Phraya River Basin, situated beneath the deltaic flood plain of the Chao Phraya River in central Thailand, is the largest groundwater basin in Thailand [1]. This basin is located in the fastest growing regions of the country, namely, the Bangkok metropolitan area and adjacent provinces. Due to rapid population growth and industrialization, the demand for groundwater for consumption has increased enormously. The total groundwater withdrawal from this basin increased from around 8,000 m^3/day in the seventies to a maximum of about 2.6 x 10^6 m^3/day in 1999 [2, 3, 4].

After the adoption of urgent mitigations actions by the local government, the groundwater withdrawal decreased again to about 10^6 m^3/day in 2008 [2, 3, 4], and to about 0.7 x 10^6 m^3/day in 2020 [5]. As the number of unregulated wells increased considerably over the past decades, the volume of groundwater actually used is likely higher than reported values [2, 3, 6]. Due to the large groundwater withdrawal, the hydraulic heads have declined from 4 meters below soil surface (bss) in the 1920s, to lower than 60 m bss in 2005 [3, 7]. This dramatic change in water table depth has reduced the size and number of open pore spaces in the aquifer system. The ground surface has undergone continuous subsidence at a rate of up to 10 cm/a in the eastern suburbs and from 5 to 10 cm/a in central Bangkok [2, 6, 8]. The uncontrolled exploitation of groundwater in the basin has led to a regional groundwater crisis, already lasting several decades and negatively affecting the country's economy and its development. Additionally, sea water intrusion in the upper aquifers of the basin has degraded the water quality in some producing wells [7, 9].

For a proper management of the groundwater resources of the basin, it is important to understand its age structure. In an earlier study, apparent radiocarbon (^{14}C, half-life: 5.7 ka) ages of groundwater in this basin were found to vary between a few thousand years in the upper aquifers, to about 40 ka in the deeper aquifers [10]. However, groundwater in several deep wells in the Bangkok region contained extremely low ^{14}C activities, close to the detection limit of the ^{14}C method. Apparent ^{14}C ages of groundwater in most of these deep wells were older than 30 ka, an age range where ^{14}C dating of groundwater is not accurate [11, 12, 13, 14]. Moreover, in this early study, only radioactive decay was considered for the interpretation of the ^{14}C data. Chemical (e.g., carbonate reactions) and physical processes in the subsurface, which are known to modify the ^{14}C activity concentrations in groundwater, were not taken into account for

the interpretation [14, 15, 16]. Furthermore, when such low ^{14}C values are analyzed, contamination during sampling or sample preparation can greatly influence the measurements [17]. Hence, apparent ^{14}C ages reported by Buapeng (1990) [10] may be significantly biased from the true age of groundwater. Sanford and Buapeng (1996) observed large discrepancies between calculated ^{14}C ages and ages simulated by backward-pathline tracking and three-dimensional groundwater flow modelling [1]. While groundwater ages based on ^{14}C were about 20 ka old, model simulations resulted in much older ages varying between 50 to 100 ka. Tanachaichoksirikun and Seeboonruang (2019) also simulated groundwater ages significantly older than those based on ^{14}C tracer data, using a steady-state three-dimensional groundwater flow model [18, 19]. In summary, significant discrepancies have been observed in the groundwater age calculated in earlier studies.

The deep aquifers in the Lower Chao Phraya River Basin likely contain water older than 30 ka. In this case, ^{81}Kr (half-life: 229 ka) is suitable for investigating, covering residence times in the range of a few hundred thousand to about one million years [20, 21, 22, 23, 24]. One of the main advantages of using ^{81}Kr is its chemical inertness, which eliminates complications that are common in interpreting ^{14}C. However, accurate detection of the ultralow levels of ^{81}Kr in groundwater has high analytical demands [25, 26, 27, 28]. This is why, despite being an ideal candidate for dating very old groundwater, this isotope had not been applied widely in the past. Only with the recent emergence of the Atom Trap Trace Analysis (ATTA) technique as a routine method for radiokrypton analysis has the number of such studies increased [27, 29, 30, 31]. For example, by using ATTA, old groundwaters have been investigated in several deep aquifers in tropical, semi-arid and arid regions [20, 22, 23, 24, 32, 33, 34].

In this study, we aimed at determining the residence time of groundwater and mixing processes in the aquifer system in the Bangkok metropolitan and vicinity areas, which is part of the Lower Chao Phraya River Basin in Thailand. As some wells in the aquifer system likely contain groundwater older than 30 ka (an age range where ^{14}C dating of groundwater is not accurate [16]), ^{81}Kr was included in this investigation. This is the first use of the ^{81}Kr tracer for obtaining insights on the structure of very old groundwater in a Thai aquifer. We present a complete data set of noble gases, including ^{81}Kr and ^{85}Kr radioisotopes, which are combined with radiocarbon, hydrogeochemical and stable isotope data. ^{81}Kr ages are used to calibrate the helium flux into the aquifer in order to utilise helium in groundwater as a quantitative age tracer. A final goal of this study is to improve our understanding of the groundwater dynamics in the Lower Chao Phraya River Basin for guiding sustainable use of this vital resource. This is particularly important because the aquifers in the basin likely contain old groundwater, which may not be renewable on human timescales [10, 18]. Tracer data produced by this study will be used in a parallel study to calibrate a groundwater flow model of the aquifer system. This model will allow an improved understanding of this complex system, and to answer important questions for water resources management in the Bangkok region.

Study area

The study area is located in the Lower Chao Phraya River Basin, which is formed by a deltaic marine plain that extends from the north boundary in Nakhon Sawan Province southward beneath the Gulf of Thailand (Figure 1). The western border of the plain is the Tanaosri mountain range. The eastern limit of the plain is the Khorat Plateau and the small hills in the Chanthaburi province. Both margins of the plain are faults scarps [35]. The plain is declining in altitude from 20 m a.s.l (meters above sea level) in the northern part to about 1.5 m a.s.l in the Bangkok area. The study area can topographically be

divided into the tidal zone, the tidal flat of marine clay, the tidal flat of brackish clay and the barrier [36].

The structure of the basement of the Bangkok plain is not well known. It has been hypothesized that block faulting in the Late Pliocene-Pleistocene dropped the Chao Phraya basement (a complex of granites and metamorphic rocks) into a graben, mainly defined by N-S faults [8]; which was filled in simultaneously as the border faulting stepped the basement down toward the axial area of the basin [8]. The geology of the Lower Central Plain consists of several structures of the depositional basin, the basement rocks of pre-Quaternary geology, and Quaternary sediments deposited in the basin [35]. The study area is composed of hard rocks of different ages in the edge of the western and eastern part of the lower central plain. The quaternary deposits are composed of unconsolidated to semi-consolidated sediments with a total thickness of 400 m to 1800 m [4, 37]. The sediments contain gravel, sand, silt and clay occurring from weathering, transportation and deposition processes. The quaternary deposits in the Lower Central Plain represent a complex sequence of alluvial, fluvial and deltaic sediments. In the Bangkok metropolitan area, seismic and boreholes (drilled for water and oil exploitation) data have showed that the depth of the basement is large and variable [8]. Granite rocks, for example, have been found as bedrocks at depths of 340 to 470 m in two recently drilled boreholes in the ridge, eastern side of the study area.

Based on electric and drilled logs data, the upper 600 m of unconsolidated alluvial deposits are subdivided into eight aquifers (Table 1, Figure 2). Thick confining clay or sandy clay layers separate them from each other [7]. The eight aquifers are treated as laterally continuous and separate; however, the interbedded clay layers are discontinuous throughout the basin and significant hydraulic connections occur between

the aquifers [8, 19, 38]. Leakages are expected over a large area as the separating clay layers are discontinue or thin out at places [8].

The Lower Chao Phraya River Basin is covered by a thick clay layer (the Bangkok clay) and vertical recharge is estimated to be low or insignificant. The recharge areas of the aquifer system are likely located along the peripheral of the basin, in the mountains, hills, terraces and alluvial fans in the western and eastern boundaries of the plain; which are about 100 km away from Bangkok [8, 9]. Natural recharge along the periphery of the basin from fractured rock basements and rainfalls and from beds of the main rivers was estimated to be 1.6 x 10^6 m^3 per day in 2004 [8].

A 15 to 30 m thick layer of blue/grey marine clay (Bangkok clay) covers the topmost unit, namely the Bangkok aquifer (BK). The BK has a depth of about 50 m. The aquifer composes of grayish-brown, fine to coarse sand with gravel and grey to greyish-brown layers [35]. The Phra Pradang aquifer (PD) has a depth of 100 m, thickness of about 20-50 m, and is composed of coarse-grained sand and gravel with clay lenses. The Nakorn Luang aquifer (NL) is formed at 100 to 140 m depth, with a thickness of 50-70 m. This unit is composed of subrounded to rounded sand and gravel with clay layers. The Nonthaburi aquifer (NB) has a similar composition to the NL unit. It is located at 170-200 m depth, and has a thickness of about 30-70 m.

The Sam Khok aquifer (SK) is located between 170-250 m depth and has thickness of about 40-80 m, consisting of medium to coarse-grained sand and gravel with intercalated clay lenses. The Phaya Thai aquifer (PT) has a depth of 275-300 m and has a thickness of about 40-60 m. This unit is composed of medium to very coarse-grained sand and gravel with clay lenses. The Thon Buri aquifer (TB), located at 350-400 m depth, has a thickness of about 50 -100 m. This aquifer consists of thick sands and gravels embedded among thin layers of clay. The sand is coarse-grained and well

sorted. Clay is generally sandy and compacted. Finally, the Pak Nam aquifer (PN), which is the lowermost unit at depths of 420-500 m, is investigated mainly in Bangkok and Samut Prakan areas. This aquifer is composed of three thick sand and gravel beds with clay lenses. Sand and gravel are white to grey and well sorted. The clay layers are compact, olive grey to dark-grey, with carbonaceous matters.

Groundwater in the Bangkok region is mostly pumped from the second (PD), third (NL), and fourth (NB) aquifers, the first one (BK) being too saline and the deeper ones necessitating excessively high drilling costs [38]. Due to the good quality and large amount of groundwater, the most pumped aquifer is NL, providing about 50% of the total groundwater extraction. Intensive groundwater exploitation has led to a steady piezometric drawdown, which has influenced subsidence and seawater intrusion in these three aquifers [8]. Seawater intrusion was identified, for example, in the northwest and southwest zones of NL and in the southern zone of PD.

The investigated area has a tropical savanna climate influenced by the monsoons [35]. The southwest monsoon season prevailing between mid-May to mid-October, the northeast monsoon season from mid-October to mid-February, and the pre-monsoon from mid-February to mid-May [35]. The mean annual air temperature (MAAT) is 27.4 ^{o}C and the average annual rainfall varies from 900 to 1450 mm [18, 39].

Methods

Field and laboratory methods

Twenty-two wells in the Bangkok aquifer system of the Lower Chao Phraya River Basin were selected for a detailed physicochemical characterization of groundwater. Two sampling campaign were conducted, the first one in January 2015 and the second one in December 2015. The wells are listed in Table 2, together with their location and

main characteristics. The works included field measurements of water electrical conductivity, pH and temperature at all the wells. Additionally, groundwater samples were collected in December 2015 for chemical (e.g., major cations and anions), tritium (^{3}H), carbon-14 (^{14}C) and carbon-13 analysis following recommended approaches [40]. Water samples for stable isotope (^{2}H, ^{18}O, and ^{13}C) analysis were collected in both sampling campaigns. The chemical composition, ^{2}H and ^{18}O (expressed in δ notations relative to VSMOW, in ‰), ^{13}C (expressed in δ notation relative to VPBD, in ‰) and ^{3}H (expressed in tritium units, TU) were analyzed at the Thailand Institute of Nuclear Technology (TINT) in Bangkok, as described elsewhere[40]. Summarizing, the chemical composition was analyzed using ion-chromatography (Dionex ICS-3000) and ICP-MS (Agilent, Model 7700), stable isotopes by laser spectrometry (Picarro L2130-I system) [41] and EA-IRMS [42]. ^{3}H was measured by liquid scintillation (Packard TriCarb 3180 TR/SL) after an enrichment step [43, 44], with a detection limit of 0.5 TU [45]. ^{14}C (expressed as percent Modern Carbon, pMC) was analyzed by Accelerator Mass Spectrometry (AMS) at the Centre for Isotope Research, University of Groningen (Netherlands), with a detection limit of about 0.5 pMC. Taking into account that apparent ages derived from low ^{14}C activities contain significant uncertainties [16], and that low ^{14}C may be as well a result of contamination during sampling and/or sample preparation [17], values below 1 pMC are not used for age calculations.

Selected wells were sampled for stable noble gases (He, Ne, Ar, Kr and Xe). The samples were collected in two field campaigns, the first one in January 2015 using 40 mL copper tubes, and the second one in December 2015 using 20 mL copper tubes. The second campaign focused on sampling the wells where samples for radioactive noble gases were collected (see below), and to re-sample some wells from the first campaign. The water samples in the copper tubes were isolated with pinch-off metal clamps to

avoid gas exchange with the atmosphere. Dissolved noble gases were extracted from the water in the copper tubes and analyzed using magnetic sector (for helium) and quadrupole (for neon, argon, krypton and xenon) mass spectrometers at the IAEA Isotope Hydrology Laboratory [46].

For radiokrypton (^{85}Kr and ^{81}Kr) analysis, dissolved gases were collected in December 2015 from eight locations using a contactor extraction method. Dissolved gases (20 - 30 L STP) were extracted from groundwater in the field and stored in pressurized cylinders. Gas samples from the pressurized cylinders were purified by cryogenic distillation, molecular sieve absorption and gas chromatography at the IAEA Isotope Hydrology Laboratory (Vienna, Austria) to produce ~10 µL (STP) sized, nearly pure krypton [47]. The abundance of radiokrypton isotopes were measured via ATTA at the Trace Radioisotope Analysis Center (TRACER), Argonne National Laboratory [29, 48]. ^{85}Kr concentrations are expressed as disintegration per minute per cm^3 Kr (dpm/ccKr). ^{81}Kr abundances are expressed in terms of the air-normalized ratio, R/R_{air}= $[^{81}Kr/Kr]_{sample}/[^{81}Kr/Kr]_{air}$, where R_{air} is the modern atmospheric ratio, $[^{81}Kr/Kr]_{air}$ = $(9.3\pm0.3) \times 10^{-13}$ [28, 31]. The R/Rair values are expressed as a percentage of the modern atmospheric value (pMKr).

Data interpretation

For the interpretation of the stable isotope data, $\delta^{18}O$ and $\delta^{2}H$ values are compared to the Bangkok local meteoric water line (LMWL: $\delta^{2}H = 7.49\ \delta^{18}O + 6.05$), the global meteoric water line (GMWL: $\delta^{2}H = 8\ \delta^{18}O + 10$), and to the long-term weighted mean annual values in Bangkok precipitation (- 6.6 ‰ for ^{18}O, and - 44.2 ‰ for ^{2}H) obtained in earlier studies [1, 10].

For the interpretation of the noble gas concentrations, the approaches described elsewhere are used [49, 50, 51]. High quality fits between the measured and modeled noble gas concentrations were obtained with the closed system equilibration (CE) model [51]. The model parameters noble gas recharge temperature (NGT) and excess air amount (expressed as % ΔNe), and the radiogenic He, were estimated in each sample.

To convert the radiogenic ^{4}He concentrations into ^{4}He model ages, the methodology presented elsewhere was applied [21, 52, 53]. Shortly, terrigenic ^{4}He concentrations are converted into groundwater ages by using a few independently determined groundwater ages from the same sample set and by using the ^{4}He distribution within a model aquifer with internal and external ^{4}He sources (an in-situ component and an external basal ^{4}He flux entering to the aquifer) [21, 52, 53, 54, 55]. This approach was demonstrated to produce ^{4}He ages in groundwater samples from Guarani aquifer [52] and from North China Plain [21] which were consistent with their respective ^{81}Kr ages.

Apparent ^{14}C ages were calculated using various models for correcting the ^{14}C initial activity [14, 56]. These models take into account different geochemical processes and can be divided into: (i) purely chemical mixing models [57], (ii) isotopic mixing models [58] and (iii) chemical mixing and isotopic exchange models [22, 59, 60, 61, 62]. ^{14}C apparent model ages are based on the following assumptions: $Ao^{14}C_{gas}$ = 100 pMC, $\delta^{13}C_{gas}$ = -23 ‰, $Ao^{14}C_{car}$ = 0 pMC, $\delta^{13}C_{car}$ = 0 ‰ [10]; where gas and car subscripts are used for the gas and carbonate phases.

The atmospheric concentration of ^{81}Kr (R_{air}) has remained relatively constant over the past few hundred [26, 28, 63, 64]. The geochemical environment under study has low uranium contents and a significant source of ^{81}Kr in the subsurface can be neglected. Consequently, variations in the isotopic ratio $^{81}Kr/Kr$ in groundwater are

assumed to be predominantly derived from radioactive decay. Using the simple expression for radioactive decay and the ^{81}Kr decay constant $\lambda = 3.03 (\pm 0.14) \times 10^{-6}$ a^{-1}, the apparent ^{81}Kr age of groundwater is calculated as reported elsewhere [20, 23].

In the atmosphere, ^{85}Kr (half-life: 10.74 a) is slightly more abundant that ^{81}Kr because of anthropogenic inputs ($[^{85}Kr/Kr]_{air} \sim 10^{-11}$). Due to its short half-life, ^{85}Kr is typically used for tracing young groundwaters, identifying air contamination during sampling or sample preparation, and/or mixing of modern with old groundwater. In this study, ^{85}Kr is used as a tracer of downward leakage of shallow modern groundwater in the wells and atmospheric contamination during sampling and Kr purification.

Results

Chemical composition

Groundwaters show a large range of variation in chemical composition (Tables 1, 2 and 3, and Figure 3). The pH of groundwater was measured in the field and ranged from 6.4 to 10.0 (Table 1). Water temperature varied in a wide range from 29 to 54 ºC (Table 1). Electrical conductivity (EC) ranged from fresh (338 µS/cm) to brackish (up to 29800 µS/cm) water types (Table 2). With the exception of the well JICA-A02 in the deep PT aquifer, saline water was found exclusively in the upper BK, PD, NL and NB aquifers, with several wells above 10 000 µS/cm. Fresh water was found at depths of more than 350 m below ground level (bgl), because of less influence of saline intrusions [9]. Most groundwaters are Na^+-Cl^-, Na^+-HCO_3^- and Ca^{2+}-HCO_3^- types, with most Na^+-Cl^- water types being found in the shallow sections of the basin above 350 m bgl (Table 3). The deeper waters in the TB and PN aquifers are Ca^{2+}-HCO_3^- and Na^+-HCO_3^- water types.

Most of the groundwater samples did not show any correlation between $Ca^{2+}+Mg^{2+}$ vs HCO_3^- or $Ca^{2+}+Mg^{2+}$ vs $HCO_3^-+SO_4^{2-}$ (Figure 3a, b), suggesting that

mineral dissolution (e.g., calcite, aragonite and dolomite) alone is likely not controlling the major ion chemistry. A clear correlation between Na^+ and Cl^- was observed (Figure 3d); indicating that dissolution of NaCl-bearing minerals and/or mixing with saline waters are the main processes responsible for the elevated Na^+ and Cl^- in groundwater. The good correlation between $[(Na^+ + K^+) - Cl^-]$ vs $[(Ca^{2+} + Mg^{2+}) - (HCO_3^- - SO_4^{2-})]$ (Figure 3c) suggests that cation exchange plays an important role in the water chemistry. This process is likely responsible for the enrichment of Ca^{2+} and Mg^{2+} compared to HCO_3^- and SO_4^{2-} in some groundwater (Figure 3a, b). Na^+ in groundwater exchanges with Ca^{2+} and Mg^{2+} on the surface of matrix minerals, resulting in increased Ca^{2+} and Mg^{2+} concentrations and decreased Na^+ concentrations in groundwater. This is for example observed in the high saline waters (e.g., JICA-A08, JICA-B04, PD-0129, NL-0129 and JICA-A02), where a high depletion in Na compared to Cl is correlated with elevated Ca and Mg concentrations. Groundwater in the south and southwest area of Bangkok city, adjacent to the Gulf of Thailand, was characterized by high concentrations of Cl^-, SO_4^{2-}, Na^+ and Mg^{2+}. This is thought to be originated by mixing of fresh water with brackish-saline water [9].

Stable isotopes

The stable isotope contents in groundwater from the aquifer system varied in a large range between -8.1 ‰ to -3.2 ‰ for $\delta^{18}O$, and from -56.7 ‰ to -24.1 ‰ for δ^2H (Table 4 and Figure 4). The groundwater samples cluster into two groups when compared to the long-term weighted mean data of stable isotopes in rainfall in Bangkok (Figure 4). A first group with $\delta^{18}O$ and δ^2H values higher than the weighted mean observed in Bangkok precipitation; and a second group, with lower isotopic values. As observed in Figure 4b, these two groundwater groups are located at different depths. In the shallower four aquifers, groundwater samples showed isotopic signatures enriched

compared to the mean isotope content for Bangkok precipitation and significantly deviating from the LMWL (Figure 4). The origin of groundwater in the shallower aquifers is likely meteoric water that has suffered evaporation and/or mixing with seawater from past intrusion [7, 9], as shown by its high Cl contents (Table 3, Figure 3d). Most of the groundwater samples from the deeper four aquifers, except samples from some wells in the SK and PT aquifers (e.g., NB-0128, SK0021, PT-0022 and JICA-A02), had depleted isotope signatures compared to the mean content in Bangkok's rainfall indicating likely recharge in colder climates. Groundwaters found at depths > 200 m (Figure 4b) likely originated from rainfall that infiltrated far from the study area, and that was only affected by recharge conditions and/or continental effects.

Tritium and radiocarbon

Tritium (^{3}H) activities in groundwater are below the detection limit of 0.5 TU (Table 4), with the exception of a sample taken in the well JICA-B02 in the NB aquifer. The detection limit for ^{3}H is below the current levels of ^{3}H in Thailand's rainfall, which range from 0.9 to 4.9 TU [44, 45]. Hence, ^{3}H activities below the detection limit indicate that a large fraction of groundwater in these aquifers is likely not of modern origin (younger than 60 a).

Radiocarbon activities and $\delta^{13}C$ values in DIC are listed in Table 4. Groundwater shows ^{14}C activities values varying between 0.6 and 65.9 pMC, and $\delta^{13}C$ between -8.2 and -21.2 ‰. Low ^{14}C activities and enriched $\delta^{13}C$ suggest long residence times of groundwater, and possibly strong equilibration with aquifer carbonate minerals [59, 60]. Some deep wells (JICA-A04, JICA-A05 and JST-002) yielded very low ^{14}C activities, approaching the detection limit for this radionuclide.

The ^{14}C activity in groundwater from the nearby-located wells JICA-A, in the eastern part of the Lower Chao Phraya Basin, shows a faster decrease with depth than in

the rest of the wells (Figure 5a). This pattern in ^{14}C activities is likely related to the existence of a different flow regime in this part of the Lower Chao Phraya River basin (Figure 1). In fact, the recharge zone of the JICA-A wells is located on the eastern flank of the basin, while the rest of the wells recharge on the western and northern flanks [1, 10]. Moreover, lower horizontal and vertical hydraulic conductivities [1] have been reported for the eastern part of the basin where the JICA-A wells are located, and this will certainly agree with a slower water flow velocities in this region. Such a slower water flow would certainly explain the ^{14}C depth profile in the JICA-A wells (Figure 5a).

In most of the investigated wells, the application of different correction models resulted in comparable apparent ^{14}C ages (Table 4). However, in four of the wells (e.g., JICA-B05, PD-129, NB-128 and SK-0021), the models resulted in significant age discrepancies. For these four wells, the apparent age calculated with the Fontes-Garnier (F-G) model was used for further interpretations. Apparent ^{14}C ages derived from the models vary between "modern" and nearly 45 ka (Table 4). The hydrological significance of apparent ^{14}C ages above 30 ka is limited, as these ages are in a range where ^{14}C dating of groundwater is not very accurate. The lower accuracy of the ^{14}C groundwater dating method when approaching the detection limit lies mainly on the fact that geochemical processes (e.g., carbonate mineral dissolution, microbial respiration, methanogenesis, diffusive mixing, etc.) that alter the ^{14}C content along the groundwater flow path would have a larger effect on the age uncertainty [16]. In addition, most of the correction models used to derive ^{14}C apparent ages contain variables that cannot be directly measured and are normally estimated or assumed [16]. This introduces additional uncertainties, which consequently affects the accuracy of ^{14}C dating method

[16]. Apparent ^{14}C ages in deep wells suggest that groundwater older than 30 ka likely exists in deep zones of the Lower Chao Phraya Basin.

Stable noble gases (He, Ne, Ar, Kr, Xe)

The parameters of the CE model (e.g., NGT and excess air) that best fitted the noble gas concentrations are reported in Table 5. In wells highly affected by salinization (e.g., JICA-A08, JICA-B-05 and JICA A-02), the model did not provide acceptable fits and therefore the fits were rejected. For the rest of the samples, the NGTs are slightly below the current MAAT of 27.4 ºC. In general, there is a tendency to find slightly warmer NGTs (typically above 20 ºC up to 28 ºC) and lower excess air concentrations (0 - 25 %) in the shallower sections of the basin (Figure 6), which contain younger groundwater. Deep wells, with older groundwater, show slightly colder NGTs (19 to 22 ºC) and higher excess air amounts (28 to 38 %) (Figure 6). The tendency observed in NGT and ΔNe likely indicates different environmental conditions during recharge in the shallow compared to the deep aquifers, as was already indicated by the $\delta^{18}O$ and $\delta^{2}H$ signatures.

Both parameters, NGT and ΔNe, have been successfully used as proxies of past climate conditions elsewhere [50, 51, 65, 66]. NGT has been linked to the mean annual air temperature in the recharge zone; and ΔNe to changes in recharge dynamics and humidity conditions produced by changes in intensity and frequency of precipitation, climatic conditions, infiltration mechanisms, etc. [51, 65, 66, 67]. For the few points in time for which data exist, our results suggest that climate conditions at recharge were in general cooler (lower NGT) and wetter (higher ΔNe: interpreted as increased number of large precipitation events) from 300 ka (Late Pleistocene) to about 10 ka (early Holocene) ago compared to those from the early Holocene to present (higher NGT and lower ΔNe). However, due to the large gaps in our dataset, this outcome should be

treated with caution. Our results are nonetheless in relative good agreement with previous studies in the region that have reported wetter and relatively unstable climatic conditions from 35 to 20 ka, and cooler and possibly drier than present climate conditions from 20 to 11.5 ka [68, 69]; then, increased precipitation for the early Holocene (12000 – 9500 a), with increased summer monsoon intensity, and a gradual decline of the intensity with warmer temperatures from mid-Holocene onwards [68].

Groundwater samples showed a large range of ^{4}He concentrations, spanning from 5×10^{-8} cm^3STP/g to 1.6×10^{-5} cm^3STP/g (Table 5). Large concentrations of ^{4}He, about two orders of magnitude higher than that of ^{4}He dissolved in the air-equilibrated water at recharge, suggest long residence times of groundwater in order to allow a significant accumulation of radiogenic ^{4}He (from the U and Th decay series) [21, 22, 70]. Indeed, the radiogenic ^{4}He component contributes significantly to the total ^{4}He in the samples, with concentrations that vary 7×10^{-9} cm^3STP/g to 1.6×10^{-5} cm^3STP/g (Table 5).

Groundwater samples with larger ^{4}He concentrations show lower $^{3}He/^{4}He$ ratios indicating that mixing of at least two isotopically distinct helium components is likely occurring. Depleted $^{3}He/^{4}He$ ratios compared to the $^{3}He/^{4}He$ ratio in atmosphere air (1.38×10^{-6}) suggest mixing with a crustal source of helium with a typical ratio of about 2×10^{-8} (Table 5). This is better observed in Figure 7, where the $^{3}He/^{4}He$ ratios are plotted against the Ne/He ratios. Plotting $^{3}He/^{4}He$ ratios versus Ne/He ratios reveals the involvement of three isotopically and elementally distinct components in the groundwater samples (Figure 7). A majority of the samples studied here plot along a two-component mixing line between atmospheric and crustal radiogenic sources. Some samples (e.g., JST-001, JICA-A03, JICA-A04 and JICA-A05) show a systematic

departure from this binary mixing trend to a source component with elevated $^{3}He/^{4}He$ and low Ne/He ratios, revealing a contribution from a mantle component (Figure 7).

While the samples JICA-A03, JICA-A04 and JICA-A05 were collected from wells located on the eastern ridge of the basin, JST-001 was collected from a well on the western ridge (Figure 1). However, all of these wells are located on the periphery of the basin (Figure 1), near faults, where helium transport from mantle rocks by upwelling may occur. For the wells located in the eastern part of the basin, a maximum contribution of about 5% mantle He is estimated (Figure 7). For the well JST-001, in the western part of the basin, a contribution of about 20% mantle He is calculated (Figure 7). Although several neighbouring wells on the periphery of the basin were sampled, only those in the deeper parts were affected by the mantle component. This is a strong indication of the deep origin of this helium component. This was the case of the samples JICA-A08, JICA-A06 and JICA-A03, which were collected from nearby wells but at different depths of 48 m, 145 m and 360 m, respectively. Only the deep sample JICA-A03 contained mantle helium.

Radiogenic ^{4}He (Table 5) shows a faster increase with depth in the eastern region where the JICA-A wells are located (Figure 5b). As discussed for ^{14}C, this pattern is likely related to the occurrence of different flow regimes in the Lower Chao Phraya River basin. The radiogenic ^{4}He data also support the occurrence of a slower water flow in the eastern part of the basin, and therefore a longer accumulation time of ^{4}He, compared to other regions of the basin.

Radiokrypton (^{85}Kr and ^{81}Kr)

In six samples (JICA-03, JICA-04, B06, PT0022, JST002 and JST001), ^{85}Kr was below 1% of modern atmospheric activity, indicating that there was no significant downward

leakage of shallow modern groundwater or atmospheric contamination during sampling and Kr purification (Table 6). In these six samples, the isotopic abundances of ^{81}Kr varied between 42 and 95 pMKr defining a broad range of apparent groundwater ages (17 to 270 ka) in the lower Chao Phraya Basin (Table 6). The sample JICA-A03, collected at about 360 m depth in the TB aquifer, showed the lowest ^{81}Kr abundance (42 ± 2 pMKr), which resulted in the oldest age approaching 300 ka (Table 6). The ^{81}Kr apparent ages represent piston flow conditions where mixing has been neglected.

The samples collected in JICA-A05 and B07 contained ^{85}Kr (activities of 3.6 and 31.4 dpm/cc), indicating that either mixing with modern groundwater components or significant contamination with atmospheric air has taken place. However, the non-detection of ^{3}H in JICA-A05 suggest a contamination with modern air. In these two samples, the isotopic abundances of ^{81}Kr were relatively high (87 and 95 pMKr), indicating relatively young apparent groundwater residence times (Table 6). The extent of the contamination with modern air can be estimated by correcting for the ^{85}Kr content in the atmosphere at the time of sampling or sampling processing, which can be assumed to be 80 dpm/cc [71, 72]. Under this assumption, we estimate a contribution of modern air of about 39% in sample B07 and of 4.5% in sample JICA-A05. This means that the original ^{81}Kr content in groundwater was 79 pMKr in B07 and 94.7 pMKr in JICA-A05. For the sample JICA-A05, the ^{81}Kr apparent age does not change significantly. However, for sample B07, an apparent age of nearly 80 ka is estimated (Table 6).

The variation of the ^{81}Kr activity with depth shows as well a regional pattern, with a faster decrease with depth in the region where the JICA-A wells are located (Figure 5b). As ^{81}Kr content in groundwater is only affected by radioactive decay, this pattern with depth is a strong indication of a slower water flow in the region where the

JICA-A wells are located than in the western and northern parts. This conclusion agrees with those obtained from the analysis of the ^{14}C and ^{4}H depth profiles (Figure 5a and 5b). Based on the variations of the ^{81}Kr apparent ages with depth, we estimate a vertical water flow velocity of 0.0533 cm a^{-1} in the eastern part of the basin, and of 0.272 cm a^{-1} in the western part of the basin. As the sampled wells are located in different aquifers, these vertical flow velocities cannot be directly converted to recharge rates.

Discussion

Insights from multiple dating tracers

Despite the large uncertainty of the ^{14}C apparent age [56], some conclusions can be drawn about the age stratification of the aquifer system. While the shallower four aquifers (BK, PD, NL and NB) contain groundwater with ^{14}C apparent ages varying between modern and about 16 ka; the deeper four aquifers (SK, PT, TB and PN) contain groundwater that span between a few thousands and more than 30 ka. Note that the ^{14}C activity in several groundwater samples approached the detection limit and apparent ages have large uncertainties [16].

In four samples (JICA-A05, PT0022, B06 and JST-002) with relatively high ^{81}Kr abundances (> 70 pMKr), ^{14}C activities significantly above the detection limit were detected (Table 6). In the samples JICA-A05 and PT0022, ^{81}Kr and ^{14}C apparent ages agree relatively well, which confirms that groundwater at those wells likely recharged about 17 ka ago at the end of the Pleistocene. For the deep wells B06 and JST-002, the residence time of groundwater based on ^{81}Kr appeared to be much older (by a factor of 4 to 6) than those obtained from ^{14}C. The large age discrepancy between these two tracers likely indicate that calculation based uniquely on assuming piston flow

conditions is not adequate for these samples. This large age difference is a strong indication that mixing of groundwater components with different ages is likely occurring at those sites and need to be taken into account [73, 74]. Groundwater mixing can potentially occur during sampling and/or due to leakage between aquifers. Sampled wells have relatively short screen intervals (< 16 m, Table 2), suggesting that mixing at sampling is probably not significant at those sites. Inter-aquifer mixing is likely the dominant mixing process. It is known that clay formations that separate the aquifers are discontinuous throughout the Lower Chao Phraya Basin, and that hydraulic connections exist between the aquifers [18, 38]. This process would certainly explain the large discrepancy between the ^{14}C and ^{81}Kr apparent ages.

The effect of groundwater mixing on tracer ages depends on the relationship between tracer concentration and age [73, 74, 75]. The concentrations of ^{14}C and ^{81}Kr decrease exponentially with age. Hence, the mean concentration of a mixed sample will not accurately reflect the mean age of the mixture but will be biased towards the younger components [73, 74, 75]. As discussed elsewhere, a larger age bias is obtained for the tracer with the shorter half-life, which is in our case ^{14}C [73, 74]. Mixing of different groundwaters is certainly the case in the wells B-06 and JST-002, where ^{14}C was detected but ^{81}Kr abundances are relatively low. ^{81}Kr dating at these two wells (B-06 and JST-002) resulted in younger ages than those calculated in samples from shallower depths (e.g., JICA-A03 and JICA-A04). This is a strong indication that mixing of younger with older groundwater is likely taking place at deep sections of the basin. Hence, calculated ^{81}Kr apparent ages at those sites are possibly younger than real groundwater ages. The effect of mixing on the calculated apparent ages varies depending on the extent of mixing and the tracer concentration in both endmembers. Due to the lack of additional data, it is not possible to further constrain this process.

Taking into account that ^{81}Kr apparent ages are less affected by mixing, we use these apparent ages as the best approximation to the groundwater ages.

In the aquifer, dissolution of atmospheric ^{4}He and accumulation of in situ produced ^{4}He (accumulation rate ~10^{-11} cm^3 STP/g/a) cannot account for the high concentrations observed in groundwater. Instead, external sources of He located in the crust can be identified based on the observed ^{3}He/^{4}He signature (Figure 7). There are good positive correlations between the concentration of terrigenic ^{4}He and apparent ^{14}C and ^{81}Kr ages (Figures 8a and 8b), supporting that concentration of terrigenic ^{4}He also has an age significance. The samples on the trends might be interpreted as a result of ^{4}He accumulation at a mean rate of about 1.9 x 10^{-11} cm^3 STP/g/a for groundwater with ^{14}C apparent ages up to 25 ka, and 3.9 x 10^{-11} cm^3 STP/g/a for older groundwaters with ^{81}Kr apparent ages older than 17 ka (Figures 8a and 8b). These accumulation rates are higher than the in-situ production of ^{4}He within the aquifer (e.g., by a decay of U and Th), confirming the existence of an external flux of ^{4}He into the aquifer most likely from underlying rocks.

For calculating ^{4}He apparent ages, two model cases are attempted, one based on ^{14}C ages (ages < 20 ka) and another one based on ^{81}Kr ages, following the methodology described elsewhere [21, 52]. The age range for ^{14}C was set to 20 ka considering the large uncertainty of older ^{14}C apparent ages. In both cases, the aquifer is assumed to have a thickness of 600 m and a porosity of 0.2 [1]. Calibration of effective ^{4}He flux (F) at the bottom of the aquifer system and vertical diffusion coefficient (D) by ^{14}C resulted in F = 9 x 10^{-7} cm^3 STP/cm^2/a and D = 1.4 x 10^{-7} m^2/sec. Figure 8c shows a comparison of the ^{14}C ages and ^{4}He model ages with these calibrated F and D. The same calibration method with ^{81}Kr ages resulted in optimum F = 7 x 10^{-7} cm^3 STP/cm^2/a and D = 1.1 x 10^{-7} m^2/sec. Figure 8d shows a comparison of ^{81}Kr ages and ^{4}He model ages with these

calibrated F and D. F and D derived from ^{81}Kr data are very similar to those estimated by ^{14}C. This was not unexpected because the range of ^{14}C ages was set to 20 ka, where an ^{4}He accumulation rate very similar to the one derived from ^{81}Kr was obtained (Fig. 8a and 8b). The ^{4}He flux across the bottom of the lower Chao Phraya Basin is about one order of magnitude smaller than the so-called crustal helium flux (~ 3 x 10^{-6} cm^3 STP/cm^2/a [52, 53]).

^{4}He model ages based on ^{14}C and ^{81}Kr apparent ages are calculated for all samples and presented in Figure 9. In most of the wells, ^{4}He model ages based on ^{14}C data tend to be younger than ^{4}He model ages based on ^{81}Kr. As indicated by ^{81}Kr ages, some groundwater samples have ages significantly older than those obtained by ^{14}C. This is likely explained by inter-aquifer mixing processes. Relatively good agreement between all tracer ages is observed at several wells (JICA-A05, PT-0022, JICA-A07, B-07), suggesting that tracer ages are representatives of groundwater ages.

Implications for the aquifer system

Our study provides evidence (e.g., chemical, stable isotopes, NGTs, excess air and tracer ages) that the aquifer system in the Bangkok and vicinity areas is stratified with depth. While the upper four aquifers contain groundwater with residence times up to a few tens of thousands of years, the deeper four aquifers contain much older groundwater up to a few hundred thousand years. Hydrogeochemical tools allowed differentiating the groundwater with depth. The stable isotope signature, recharge temperature and excess air component suggested that groundwater from the shallower aquifers recharged at different environmental conditions (e.g., climate, location, etc.) than groundwater found in the deeper aquifers. Moreover, numerous wells in the shallower aquifers contain highly saline groundwater likely because of mixing with

brines from past saline intrusion. Deep aquifers contain in general high-quality old groundwater.

The tracer data (^{81}Kr and ^{14}C) at several sites in the investigated area evidenced, nonetheless, that leakage between aquifers is taking place. Inter-aquifer mixing may have important implications (locally and/or regionally) on the degree of stratification of the aquifer system, and therefore on the water quality. Unfortunately, due to the lack of geological data, it was not possible to further constrain this process here. The identification of inter-aquifer mixing is an important outcome, especially from a management point of view. Moreover, it is plausible that enhanced inter-aquifer leakage could occur at other locations across the basin, and needs to be investigated in the future.

The depth profiles of ^{14}C, ^{4}He and ^{81}Kr showed consistent regional patterns likely related to different regional water flow regimes in the Lower Chao Phraya River Basin. Our data indicates that water flows much slower in the eastern part of the basin, where the JICA-A wells are located, than in the western part. As a consequence, the groundwater renewal time in this region of the Lower Chao Phraya River Basin is slower than in other part of the basin.

Conclusions

Radioactive and stable isotopes and chemical tracers were applied in the complex aquifer system forming the Lower Chao Phraya River Basin to determine groundwater age. Through this study, the groundwater age in deep aquifers of the Lower Chao Phraya River Basin was estimated for the first time. ^{81}Kr revealed apparent ages spanning from 17 to 300 ka, demonstrating that natural groundwater replenishment occurs even more slowly than previously thought. The use of ^{14}C was mostly limited to

the upper four aquifers of the basin, because ^{14}C activities were approaching the detection limit in the deeper aquifers. Low or negligible ^{14}C activities further confirmed the presence of groundwater older than 30 ka. ^{81}Kr dating of groundwater from the Bangkok area shed new light on the age structure of this system, which was previously assessed as a seemingly homogeneous distribution of ^{14}C ages. Elevated ^{4}He concentrations, varying in about two orders of magnitude, also reflected large accumulation times in the subsurface. Hence, all residence time indicators confirmed the presence of very old groundwater in the deeper aquifers of the Lower Chao Phraya Basin. Moreover, the tracer data evidenced that inter-aquifer mixing is a relevant process in deep sections of this basin. Hence, any future development should be accompanied by a local-scale assessment of the nature of the inter-aquifer leakage. Finally, the combined use of ^{14}C, ^{4}He and ^{81}Kr allowed to identify different flow regimes in the Lower Chao Phraya River Basin. These tracers simultaneously confirmed a slower water flow velocity in the eastern part of the basin compared to other areas. This result has important implications for water resources management in this region.

This study further demonstrated that water quality in the Lower Chao Phraya River Basin varies strongly with depth. While younger water with signs of salinization by seawater intrusions (brackish water) was found in the upper aquifers, older and good quality water (fresh water) was found in the deeper aquifers. As this very old and good quality water found in the Bangkok region will not be replenished on a human timescale, exploitation would need to be regulated in order to guarantee a sustainable management of this limited resource. Overpumping this non-renewable groundwater may contribute to groundwater shortage in the future. Moreover, groundwater pumping must be carefully managed, because it may cause land subsidence and seawater intrusion.

Acknowledgment

We thank the International Atomic Energy Agency for funding this study under the Technical Cooperation Project THA-16879. KK, MY, CS, PC, CP and NU were supported by the Thailand Institute of Nuclear Technology. JACA was supported by Spiez Laboratory, Swiss Federal Office for Civil Protection. OO, VH and AW were supported by the Department of Groundwater Resources of the Thailand Ministry of Natural Resources and Environment. JCZ and PM were supported by the US Department of Energy, Office of Nuclear Physics, under contract DE-AC02-06CH11357.

Conflict of Interest

The authors declare that they have no conflict of interest.

References

1. Sanford WE, Buapeng S. Assessment of a groundwater flow model of the Bangkok Basin, Thailand, using Carbon-14-based ages and paleohydrology. Hydrogeology Journal. 1996;4(4):26-40. doi: 10.1007/s100400050083.
2. Buapeng S, Wattayakorn G. Groundwater situation in Bangkok and its vicinity. From headwaters to the ocean hydrological changes and watershed management Kyoto, Japan, 2008.
3. Buapeng S, Foster S. Controlling groundwater abstraction and related environmental degradation in metropolitan Bangkok – Thailand, 2008.
4. Lorphensri O, Ladawadee A, Dhammasarn S. Review of groundwater management and land subsidence in Bangkok, Thailand. In: Taniguchi M, editor. Groundwater and subsurface environments: human impacts in Asian coastal cities. Tokyo: Springer Japan; 2011. p. 127-142.
5. Tanachaichoksirikun P, Seeboonruang U, Fogg GE. Improving groundwater model in regional sedimentary basin using hydraulic gradients. KSCE Journal of Civil Engineering. 2020;24(5):1655-1669. doi: 10.1007/s12205-020-1781-8.
6. Intui S, Inazumi S, Soralump S. Evaluation of land subsidence during groundwater recovery. Applied Sciences. 2022;12(15):7904. PubMed PMID: doi:10.3390/app12157904.
7. Ramnarong V, Buapeng S. Saltwater intrusion and land subsidence due to over exploitation of groundwater in Bangkok. International Geological Congress1992.

8. Phien-wej N, Giao PH, Nutalaya P. Land subsidence in Bangkok, Thailand. Engineering Geology. 2006;82(4):187-201. doi: https://doi.org/10.1016/j.enggeo.2005.10.004.
9. Stoecker F, Babel MS, Gupta AD, et al. Hydrogeochemical and isotopic characterization of groundwater salinization in the Bangkok aquifer system, Thailand. Environmental Earth Sciences. 2013;68(3):749-763. doi: 10.1007/s12665-012-1776-y.
10. Buapeng S. The use of environmental isotopes on groundwater hydrology in the selected areas in Thailand. In: IAEA, editor. Vienna, Austria1990. p. 76.
11. Cartwright I, Cendón D, Currell M, et al. A review of radioactive isotopes and other residence time tracers in understanding groundwater recharge: Possibilities, challenges, and limitations. Journal of Hydrology. 2017;555:797-811. doi: https://doi.org/10.1016/j.jhydrol.2017.10.053.
12. Cartwright I, Fifield LK, Morgenstern U. Using ^{3}H and ^{14}C to constrain the degree of closed-system dissolution of calcite in groundwater. Applied Geochemistry. 2013;32:118-128. doi: https://doi.org/10.1016/j.apgeochem.2012.10.023.
13. Clark I. Groundwater Geochemistry and Isotopes (1st ed.). Boca Raton: CRC Press.
14. Han LF, Plummer LN. A review of single-sample-based models and other approaches for radiocarbon dating of dissolved inorganic carbon in groundwater. Earth-Science Reviews. 2016;152:119-142. doi: https://doi.org/10.1016/j.earscirev.2015.11.004.
15. Han L-F, Plummer LN, Aggarwal P. A graphical method to evaluate predominant geochemical processes occurring in groundwater systems for radiocarbon dating. Chemical Geology. 2012;318-319:88-112. doi: https://doi.org/10.1016/j.chemgeo.2012.05.004.
16. Han L-F, Wassenaar LI. Principles and uncertainties of 14C age estimations for groundwater transport and resource evaluation. Isotopes in Environmental and Health Studies. 2021;57(2):111-141. doi: 10.1080/10256016.2020.1857378.
17. Aggarwal PK, Araguas-Araguas L, Choudhry M, et al. Lower Groundwater 14C Age by Atmospheric CO2 Uptake During Sampling and Analysis. Groundwater. 2014;52(1):20-24. doi: https://doi.org/10.1111/gwat.12110.
18. Tanachaichoksirikun P, Seeboonruang U. Distributions of groundwater age under climate change of Thailand's Lower Chao Phraya Basin. Water. 2020;12(12):3474. PubMed PMID: doi:10.3390/w12123474.
19. Tanachaichoksirikun P, Seeboonruang U. Effect of climate change on groundwater age of Thailand's Lower Chao Phraya Basin. IOP Conference Series: Materials Science and Engineering. 2019;639(1):012032. doi: 10.1088/1757-899X/639/1/012032.
20. Gerber C, Vaikmäe R, Aeschbach W, et al. Using 81Kr and noble gases to characterize and date groundwater and brines in the Baltic Artesian Basin on the one-million-year timescale. Geochimica et Cosmochimica Acta. 2017;205:187-210. doi: https://doi.org/10.1016/j.gca.2017.01.033.
21. Matsumoto T, Chen Z, Wei W, et al. Application of combined 81Kr and 4He chronometers to the dating of old groundwater in a tectonically active region of the North China Plain. Earth and Planetary Science Letters. 2018;493:208-217. doi: https://doi.org/10.1016/j.epsl.2018.04.042.
22. Matsumoto T, Zouari K, Trabelsi R, et al. Krypton-81 dating of the deep Continental Intercalaire aquifer with implications for chlorine-36 dating. Earth

and Planetary Science Letters. 2020;535:116120. doi: https://doi.org/10.1016/j.epsl.2020.116120.
23. Sturchio NC, Du X, Purtschert R, et al. One million year old groundwater in the Sahara revealed by krypton-81 and chlorine-36. Geophysical Research Letters. 2004;31(5). doi: 10.1029/2003gl019234.
24. Yokochi R, Zappala JC, Purtschert R, et al. Origin of water masses in Floridan Aquifer System revealed by 81Kr. Earth and Planetary Science Letters. 2021;569:117060. doi: https://doi.org/10.1016/j.epsl.2021.117060.
25. IAEA. Isotope methods for dating old groundwater. Vienna, Austria 2013.
26. Collon P, Antaya T, Davids B, et al. Measurement of 81Kr in the atmosphere. Nuclear Instruments and Methods in Physics Research Section B: Beam Interactions with Materials and Atoms. 1997;123(1):122-127. doi: https://doi.org/10.1016/S0168-583X(96)00674-X.
27. Jiang W, Hu S-M, Lu Z-T, et al. Latest development of radiokrypton dating – A tool to find and study paleogroundwater. Quaternary International. 2020;547:166-171. doi: https://doi.org/10.1016/j.quaint.2019.04.025.
28. Purtschert R, Yokochi R, Jiang W, et al. Underground production of 81Kr detected in subsurface fluids. Geochimica et Cosmochimica Acta. 2021;295:65-79. doi: https://doi.org/10.1016/j.gca.2020.11.024.
29. Jiang W, Bailey K, Lu ZT, et al. An atom counter for measuring 81Kr and 85Kr in environmental samples. Geochimica et Cosmochimica Acta. 2012;91:1-6. doi: https://doi.org/10.1016/j.gca.2012.05.019.
30. Zappala JC, Bailey K, Jiang W, et al. Setting a limit on anthropogenic sources of atmospheric 81Kr through Atom Trap Trace Analysis. Chemical Geology. 2017;453:66-71. doi: https://doi.org/10.1016/j.chemgeo.2017.02.007.
31. Zappala JC, Baggenstos D, Gerber C, et al. Atmospheric 81Kr as an Integrator of Cosmic-Ray Flux on the Hundred-Thousand-Year Time Scale. Geophysical Research Letters. 2020;47(3):e2019GL086381. doi: https://doi.org/10.1029/2019GL086381.
32. Sturchio NC, Kuhlman KL, Yokochi R, et al. Krypton-81 in groundwater of the Culebra Dolomite near the Waste Isolation Pilot Plant, New Mexico. Journal of Contaminant Hydrology. 2014;160:12-20. doi: https://doi.org/10.1016/j.jconhyd.2014.02.002.
33. Yokochi R, Ram R, Zappala JC, et al. Radiokrypton unveils dual moisture sources of a deep desert aquifer. Proceedings of the National Academy of Sciences. 2019;116(33):16222-16227. doi: 10.1073/pnas.1904260116.
34. Vives L, Rodríguez L, Manzano M, et al. Using isotope data to characterize and date groundwater in the southern sector of the Guaraní Aquifer System. Isotopes in Environmental and Health Studies. 2020;56(5-6):533-550. doi: 10.1080/10256016.2020.1810684.
35. Sinsakul S. Late Quaternary geology of the Lower Central Plain, Thailand. Journal of Asian Earth Sciences. 2000;18(4):415-426. doi: https://doi.org/10.1016/S1367-9120(99)00075-9.
36. JICA KKLa. The Study on Management of Groundwater and Land Subsidence in the Bangkok Metropolitan Area and its Vicinity. Final Report.: Japan International Cooperation Agency (JICA); 1995.
37. Kogyo K. The study on management of groundwater and land subsidence in the Bangkok metropolitan area and its vicinity. In: Agency JIC, editor. Tokyo, Japan, 1995.

38. Bremard T. Monitoring Land Subsidence: The Challenges of Producing Knowledge and Groundwater Management Indicators in the Bangkok Metropolitan Region, Thailand. Sustainability. 2022;14(17):10593. PubMed PMID: doi:10.3390/su141710593.
39. Putthividhya A, Laonamsai J. Hydrological assessment using stable isotope fingerprinting technique in the Upper Chao Phraya river basin. Lowland Technology International. 2017;19:27-40.
40. Kamdee K, Corcho Alvarado JA, Occarach O, et al. Application of isotope techniques to study groundwater resources in the unconsolidated aquifers along the Ping River (Thailand). Isotopes in Environmental and Health Studies. 2020:1-16. doi: 10.1080/10256016.2020.1739672.
41. Busch KW, Busch MA. Cavity-ringdown spectroscopy : an ultratrace-absorption measurement technique. Vol. 720. 1999.
42. TECDOC-1723: Using isotopes for design and monitoring of artificial recharge systems. Vienna: IAEA; 2013.
43. Rozanski K, Groening M. Tritium assay in water samples using electrolytic enrichment and liquid scintillation spectrometry. In: IAEA, editor. Vienna, Austria, 2004. p. 195-217.
44. Khamanek K, Khuntong S, Saenboonruang K, et al. Assessing tritium contamination in Thailand's rainwater: A study of environmental monitoring and nuclear surveillance. Journal of Environmental Radioactivity. 2023;262:107151. doi: https://doi.org/10.1016/j.jenvrad.2023.107151.
45. Kamdee K, Srisuk K, Lorphensri O, et al. Use of isotope hydrology for groundwater resources study in Upper Chi river basin. J Radioanal Nucl Chem Art. 2013;297. doi: 10.1007/s10967-012-2401-y.
46. Matsumoto T, Solomon DK, Araguás-Araguás L, et al. The IAEA's Coordinated Research Project on "Estimation of groundwater recharge and discharge by using the Tritium, Helium-3 dating technique". Geochemical Journal. 2017;51(5):385-390. doi: 10.2343/geochemj.2.0500.
47. Hillegonds D, Matsumoto T, Romeo N. Krypton isolation and purification from groundwater for 81Kr age dating. International Symposium on Isotope Hydrology: Revisiting Foundations and Exploring Frontiers. 2015:49.
48. Lu Z-T, Mueller P. Chapter 4 - Atom Trap Trace Analysis of Rare Noble Gas Isotopes. In: Berman P, Arimondo E, Lin C, editors. Advances In Atomic, Molecular, and Optical Physics. 58: Academic Press; 2010. p. 173-205.
49. Aeschbach-Hertig W, El-Gamal H, Wieser M, et al. Modeling excess air and degassing in groundwater by equilibrium partitioning with a gas phase. Water Resources Research. 2008;44(8). doi: doi:10.1029/2007WR006454.
50. Aeschbach-Hertig W, Peeters F, Beyerle U, et al. Palaeotemperature reconstruction from noble gases in ground water taking into account equilibration with entrapped air. Nature. 2000;405:1040. doi: 10.1038/35016542.
51. Aeschbach-Hertig W, Peeters F, Beyerle U, et al. Interpretation of dissolved atmospheric noble gases in natural waters. Water Resources Research. 1999;35(9):2779-2792. doi: doi:10.1029/1999WR900130.
52. Aggarwal PK, Matsumoto T, Sturchio NC, et al. Continental degassing of 4He by surficial discharge of deep groundwater. Nature Geoscience. 2015;8(1):35-39. doi: 10.1038/ngeo2302.
53. Castro MC, Stute M, Schlosser P. Comparison of 4He ages and 14C ages in simple aquifer systems: implications for groundwater flow and chronologies.

Applied Geochemistry. 2000;15(8):1137-1167. doi: https://doi.org/10.1016/S0883-2927(99)00113-4.
54. Torgersen T, Ivey GN. Helium accumulation in groundwater. II: A model for the accumulation of the crustal 4He degassing flux. Geochimica et Cosmochimica Acta. 1985;49(11):2445-2452. doi: https://doi.org/10.1016/0016-7037(85)90244-3.
55. Aggarwal PK, Chang HK, Gastmans D, et al. Krypton-81, Helium-4 and Carbon-14 based estimation of groundwater ages in the Guarani Aquifer System: implications for the He-4 geochronometer. American Geophysical Union, Fall Meeting; December 01, 20122012. p. H12A-05.
56. Han L-F, Plummer LN. Revision of Fontes & Garnier's model for the initial 14C content of dissolved inorganic carbon used in groundwater dating. Chemical Geology. 2013;351:105-114. doi: https://doi.org/10.1016/j.chemgeo.2013.05.011.
57. Tamers MA. Validity of radiocarbon dates on ground water. Geophysical Surveys. 1975;2(2):217-239. doi: 10.1007/BF01447909.
58. Ingerson E, Pearson F. Estimation of age and rate of motion of groundwater by the 14C-method. Recent researches in the fields of atmosphere, hydrosphere and nuclear geochemistry. 1964:263-283.
59. Fontes JC, Garnier JM. Determination of the initial 14C activity of the total dissolved carbon: A review of the existing models and a new approach. Water Resources Research. 1979;15(2):399-413. doi: 10.1029/WR015i002p00399.
60. Mook WG. The dissolution-exchange model for dating groundwater with 14C. Vienna, Asutria: IAEA; 1976.
61. Salem O, Visser J, Dray M, et al. Groundwater flow patterns in the western Libyan Arab Jamahiriya evaluated from isotopic data. Advisory group meeting on application of isotope techniques in arid zones hydrology. Vienna, Austria: IAEA; 1980.
62. Eichinger L. A contribution to the interpretation of 14C groundwater ages considering the example of a partially confined sandstone aquifer. Radiocarbon. 1983;25(2):347-356.
63. Loosli HH, Oeschger H. 37Ar and81Kr in the atmosphere. Earth and Planetary Science Letters. 1969;7(1):67-71. doi: https://doi.org/10.1016/0012-821X(69)90014-4.
64. Aalseth CE, Day AR, Fuller ES, et al. A new shallow underground gas-proportional counting lab—First results and Ar-37 sensitivity. Appl Radiat Isot. 2013;81(0):151-155. doi: http://dx.doi.org/10.1016/j.apradiso.2013.03.050.
65. Aeschbach-Hertig W, Solomon DK. Noble Gas Thermometry in Groundwater Hydrology. In: Burnard P, editor. The Noble Gases as Geochemical Tracers. Berlin, Heidelberg: Springer Berlin Heidelberg; 2013. p. 81-122.
66. Seltzer AM, Ng J, Aeschbach W, et al. Widespread six degrees Celsius cooling on land during the Last Glacial Maximum. Nature. 2021;593(7858):228-232. doi: 10.1038/s41586-021-03467-6.
67. Corcho Alvarado JA, Leuenberger M, Kipfer R, et al. Reconstruction of past climate conditions over central Europe from groundwater data. Quaternary Science Reviews. 2011;30(23–24):3423-3429. doi: http://dx.doi.org/10.1016/j.quascirev.2011.09.003.
68. White JC, Penny D, Kealhofer L, et al. Vegetation changes from the late Pleistocene through the Holocene from three areas of archaeological

significance in Thailand. Quaternary International. 2004;113(1):111-132. doi: https://doi.org/10.1016/j.quaint.2003.09.001.
69. Suraprasit K, Shoocongdej R, Chintakanon K, et al. Late Pleistocene human paleoecology in the highland savanna ecosystem of mainland Southeast Asia. Scientific reports. 2021;11(1):16756-16756. doi: 10.1038/s41598-021-96260-4. PubMed PMID: 34408215; eng.
70. Corcho Alvarado JA, Pačes T, Purtschert R. Dating groundwater in the Bohemian Cretaceous Basin: Understanding tracer variations in the subsurface. Applied Geochemistry. 2013;29:189-198. doi: https://doi.org/10.1016/j.apgeochem.2012.11.014.
71. Kersting A, Brander S, Suckow A. Modelling (85)Kr datasets with python for applications in tracer hydrology and to investigate atmospheric circulation. MethodsX. 2021;8:101245-101245. doi: 10.1016/j.mex.2021.101245. PubMed PMID: 34434768; eng.
72. Kersting A, Schlosser C, Bollhöfer A, et al. Evaluating 5 decades of atmospheric 85Kr measurements in the southern hemisphere to derive an input function for dating water and ice with implications for interhemispheric circulation and the global 85Kr emission inventory. Journal of Environmental Radioactivity. 2020;225:106451. doi: https://doi.org/10.1016/j.jenvrad.2020.106451.
73. Suckow A. The age of groundwater – Definitions, models and why we do not need this term. Applied Geochemistry. 2014;50:222-230. doi: https://doi.org/10.1016/j.apgeochem.2014.04.016.
74. Bethke CM, Johnson TM. Groundwater age and groundwater age dating. Annual Review of Earth and Planetary Sciences. 2008;36(1):121-152. doi: 10.1146/annurev.earth.36.031207.124210.
75. Cook P. Introduction to Isotopes and Environmental Tracers as Indicators of Groundwater Flow. Ontario, Canada: The Groundwater Project; 2020.

Table 1. The main aquifers in the lower Chao Phraya River Basin.

Aquifer	Depth (m)	Groundwater	Lithology
Bangkok - BK	~50	Saline Brackish	Fine to coarse sand with gravel
Phra Pradaeng - PD	50-100	Saline Brackish	Coarse-grained sand and gravel with clay lenses
Nakhon Luang - NL	100-140	Saline Brackish	Sand and gravel with clay layers
Nontha Buri - NB	170-200	Saline Brackish	Sand and gravel with clay layers
Sam Khok – SK	170-250	Fresh	Medium to coarse-grained sand and gravel with intercalated clay lenses
Phaya Thai – PT	275-300	Fresh	Coarse-grained sand and gravel with clay lenses
Thon Buri – TB	350-450	Fresh	Thick sand and gravel embedded among thin layers of clay
Pak Nam - PN	420-500	Fresh	Thick sand and gravel beds with clay lenses

Table 2. Information about the sampled wells in the lower Chao Phraya River Basin and some physico-chemical properties of groundwater. Electrical conductivity (EC), pH and Temperature (T) data for January (Jan) and December (Dec) 2015 are reported.

Well	Aquifer	Location		Depth	Screen interval	Water level	EC (µS)		pH		T (ºC)	
		East	North	(m)	(m)	(m)	Jan	Dec	Jan	Dec	Jan	Dec
JICA-A08	BK	687617	1521775	48	41-47	11.23	>4000	29800	8.4	5.2	31.4	30.2
JICA-B05		674037	1557553	47	41-47	4.73	>4000	17800	7.7	7.3	29.9	30.1
JICA-B04	PD	674037	1557553	94	88-94	18.43	>4000	6030	8.0	6.5	30.0	30.0
JICA-A06	NL	687617	1521775	145	136-144	21.16	723	667	8.4	8.9	30.7	32.5
JICA-A07		687599	1521797	108	101-107	17.92	1188	1200	10.0	9.3	29.7	30.5
PD-0129		652547	1526141	121	110-118	16.76	3215	12100	6.4	6.4	30.7	31.2
JICA-B02	NB	674037	1557553	192	186-192	20.81	750	763	8.4	7.8	29.8	31.1
JICA-B03		674037	1557553	153	147-153	19.28	1940	2050	7.3	7.8	30.9	30.8
NL-0129		652547	1526141	163	152-160	18.92	2817	10100	6.6	6.6	29.5	30.1
JICA-A05	SK	687599	1521797	215	206-214	20.78	1093	1080	9.9	8.8	34.1	32.3
JICA-B01		674037	1557553	272	263-272	47.16	983	879	7.7	8.2	33.7	31.5
NB-0128		652547	1526141	220	208-216	21.34	516	767	8.0	7.6	34.1	31.2
SK-0021		652547	1526141	261	252-258	21.44	595	1010	9.6	8.0	29.8	30.4
PT-0022		652547	1526141	309	300-306	22.43	546	809	6.6	7.8	29.9	31.4
JICA-A02	PT	687599	1521797	437	428-436	31.41	>4000	28400	6.8	6.6	31.2	31.0
JICA-A04		687628	1521792	302	293-301	25.04	1439	1510	9.7	8.4	33.5	33.9
JICA-A03	TB	687617	1521775	360	351-359	26.31	1042	994	10.5	9.5	32.6	33.2
JST- 001		644185	1507709	420	402-420	-	338	401	7.3	8.0	54.0	50.9
JICA-A01	PN	687628	1521792	574	558-574		1734	1980	9.8	9.9	32.6	31.8
B-06		658539	1553049	650	-	-	498	457	8.5	8.1	41.2	47.0
B-07		658218	1553399	575	-	-	408	398	8.4	7.8	41.9	49.5
JST-002		656013	1507312	605	558-605	-	636	906	7.6	7.9	46.0	50.1

Table 3. Results of the chemical analysis of the groundwater samples collected in the lower Chao Phraya River basin.

Well	Aquifer	Ca	Mg	Na	K	SO_4	Cl	CO_3	HCO_3	NO_3
						mg L^{-1}				
JICA-A08	BK	1100	280	5000	45	240	11000	0	30	< 0.9
JICA-B05		150	360	3400	48	130	6200	0	201	< 0.9
JICA-B04	PD	380	150	620	8.8	< 1	2000	0	13	< 0.9
JICA-A06	NL	1	6.8	160	2	< 1	4.8	41	371	< 0.9
JICA-A07		2	3.6	260	2.8	22	260	24	179	< 0.9
PD-0129		380	300	1800	40	300	4200	0	118	< 0.9
JICA-B02	NB	52	15	83	8.8	< 1	83	0	339	< 0.9
JICA-B03		74	42	310	4.7	< 1	550	0	274	< 0.9
NL-0129		580	270	1100	24	200	3300	0	181	< 0.9
JICA-A05	SK	1.2	4.6	230	1.3	60	190	11	189	< 0.9
JICA-B01		4	8.9	160	5.5	< 1	190	0	170	< 0.9
NB-0128		60	10	86	3.3	6	87	0	340	< 0.9
SK-0021		10	24	160	7.3	< 1	270	0	86	< 0.9
PT-0022		47	14	110	4.1	10	94	0	344	< 0.9
JICA-A02	PT	1300	610	4200	41	47	11000	0	18	< 0.9
JICA-A04		4.4	8	340	1.3	73	290	13	275	< 0.9
JICA-A03	TB	0.00	3.6	240	0.60	13	57	82	368	< 0.9
JST- 001		43	19	6	8.8	< 1	5.6	0	251	< 0.9
JICA-A01	PN	0.8	0.5	450	2.1	280	190	128	220	< 0.9
B-06		35	8.9	43	5.7	2	30	0	241	< 0.9
B-07		32	11	30	5.7	< 1	12	0	236	< 0.9
JST-002		26	9.6	150	6.4	32	130	0	286	< 0.9

Table 4. Stable isotopes, ^{14}C, ^{13}C and ^{3}H data in groundwater samples collected in the lower Chao Phraya River basin. For the stable isotopes, data from January (Jan) and December (Dec) 2015 and their respective deuterium excesses (d-exc. = $\delta^{2}H - 8 * \delta^{18}O$) are reported.

Well	$\delta^{18}O$ (‰)		$\delta^{2}H$ (‰)		d-exc. (‰)	d-exc. (‰)	^{3}H (TU)	$\delta^{13}C$ (‰)	^{14}C (pMC)	^{14}C apparent ages (a) Model				
	Jan	Dec	Jan	Dec	Jan	Dec		(VPBD)	Dec	Tamers	Pearson	Mook	F-G	IAEA
JICA-A08	-3.4	-3.2	-24.9	-24.1	2.3	1.3	< 0.5	-21.2	39.1 ± 1.4	7492	7110	6377	7090	10313
JICA-B05	-5.1	-5.1	-35.3	-35.3	5.5	5.4	< 0.5	-10.7	52.6 ± 1.5	279	Modern	Modern	Modern	2131
JICA-B04	-6.0	-6.0	-43.2	-43.2	4.6	4.5	< 0.5	-10.9	n.a.					
JICA-A06	-4.8	-4.7	-36.0	-35.8	2.3	1.8	< 0.5	-10.9	6.8 ± 0.1	16514	16050	15224	16022	19128
JICA-A07	-5.8	-5.7	-42.1	-42.0	4.3	4.0	< 0.5	-	5.1 ± 0.1	18880				
PD-0129	-5.4	-5.3	-39.8	-38.7	3.8	3.5	< 0.5	-12.0	27.2 ± 0.2	8138	5385	Modern	5204	8533
JICA-B02	-5.5	-5.7	-46.0	-44.8	-1.6	0.4	1.0	-11.1	65.9 ± 0.3	Modern	Modern	Modern	Modern	579
JICA-B03	-4.4	-4.2	-34.3	-33.4	1.2	0.5	< 0.5	-11.1	14.2 ± 1.1	10787	10230	9153	10199	13401
NL-0129	-5.0	-4.8	-37.2	-35.2	3.1	3.5	< 0.5	-9.6	19.7 ± 1.1	10045	6082		5811	9290
JICA-A05	-7.1	-7.0	-50.4	-50.2	6.3	5.5	< 0.5	-14.9	3.2 ± 0.1	*22751*	*24865*	*27491*	*25670*	*27954*
JICA-B01	-6.9	-7.1	-50.1	-50.5	5.2	6.1	n.a.	-	20.6 ± 0.2	7438				
NB-0128	-5.1	-5.2	-37.9	-37.9	2.7	3.4	< 0.5	-8.2	20.7 ± 0.2	7695	4494	Modern	4277	7643
SK-0021	-5.4	-5.3	-41.6	-40.2	1.9	1.8	n.a.	-10.8	35.8 ± 0.2	2932	2243	850	2204	5435
PT-0022	-5.4	-5.3	-41.1	-40.6	2.4	1.8	n.a.	-14.8	16.3 ± 0.1	9528	11351	13767	12074	14489
JICA-A02	-4.2	n.a.	-30.5	n.a.	3.5	-	n.a.	-15.4	40.6 ± 1.7	4099	4055	3977	4052	7214
JICA-A04	-7.5	-7.4	-53.2	-52.8	7.1	6.5	n.a.	-18.3	0.60 ± 0.03					
JICA-A03	-7.8	-7.8	-54.7	-54.6	7.3	7.5	n.a.	-14.7	< 0.5					
JST- 001	-7.2	-7.0	-49.0	-48.7	8.2	7.7	n.a.	-12.5	n.a.					
JICA-A01	-7.9	-8.1	-55.7	-56.7	7.8	8.0	n.a.	-9.6	<0.5					
B-06	-7.4	-7.2	-53.0	-52.5	5.9	5.3	n.a.	-10.7	9.9 ± 0.1	13512	12792	12006	12724	15163
B-07	-7.4	-7.3	-53.4	-53.2	6.1	5.5	n.a.	-11.1	n.a.					
JST-002	-7.4	-7.3	-53.1	-53.2	5.7	5.3	n.a.	-12.8	3.6 ± 1.2	*21944*	*22636*	*23213*	*22839*	*24871*

n.a.: not analyzed

Table 5. Noble gas data and results of their interpretation with the closed system equilibration (CE) model. Samples collected in (1) January 2015 and in (2) December 2015 are reported. #Note that terrigenic ^{4}He was calculated by applying the CE model using a recharge altitude of 200 m, which corresponds to a mean altitude in the recharge zone. Selection of the altitude should not affect the resultant ^{4}He model ages to a significant extent, but might have induced some systematic shift in the ^{4}He model ages.

Sample	He 10^{-7}	Ne 10^{-7}	Ar 10^{-4} (cm^3STP/g)	Kr 10^{-8}	Xe 10^{-9}	^{3}He/^{4}He 10^{-7}	Depth (m)	χ^2	Prob. (%)	NGT (°C)	Exc. air (% ΔNe)	Exc.^{4}He # 10^{-7} (cm^3STP/g)
JICA-A08	0.5	0.8	14.7	-	-	6.6	48	-	-	-	-	-
JICA-B05	0.7	1.4	2.2	4.9	6.2	7.5	47	-	-	-	-	-
JICA-B04	1.9	2.2	3.4	6.9	7.6	6.3	94	10.3	0.6	21.1 ± 1.4	22	1.37 ± 0.06
JICA-A06	2.2	2.3	3.2	5.8	7.2	4.4	145	10.6	0.5	26.8 ± 1.4	35	1.59 ± 0.05
JICA-A07	0.9	1.7	2.8	6.2	7.7	9.3	108	2.4	30.0	25.0 ± 1.4	0	0.47 ± 0.03
PD-0129	0.6	1.9	2.8	5.8	6.8	10.7	121	2.3	31.9	27.9 ± 1.5	12	0.07 ± 0.02
JICA-B02 (2)	1.7	1.7	2.7	5.7	7.1	2.0	192	9.7	0.8	27.3 ± 0.4	1	1.22 ± 0.02
JICA-B03	1.5	2.2	3.4	6.7	8.0	5.3	153	5.4	6.8	21.2 ± 1.4	24	0.92 ± 0.04
NL-0129 (2)	1.0	2.2	3.0	6.3	7.6	7.0	163	1.1	57.8	25.6 ± 1.4	26	0.46 ± 0.03
JICA-A05	6.8	2.0	2.8	6.1	7.3	3.9	215	0.9	64.7	26.6 ± 1.5	15	6.3 ± 0.2
JICA-B01	8.8	2.3	3.4	7.1	8.5	1.7	272	2.6	27.8	20.9 ± 1.2	31	8.2 ± 0.3
NB-0128	1.4	2.5	3.5	7.4	9.1	8.2	220	2.2	32.9	19.1 ± 1.2	37	0.74 ± 0.04
SK-0021	1.2	1.8	3.0	6.2	8.3	5.2	264	3.4	18.5	22.4 ± 0.7	2	0.70 ± 0.02
PT-0022	7.5	2.4	3.5	6.6	8.5	1.3	309	5.1	7.6	21.1 ± 1.4	34	6.9 ± 0.2
JICA-A02	0.5	0.9	1.6	3.6	4.4	6.5	437	-	-	-	-	-
JICA-A04	32	2.3	3.3	6.7	8.6	6.0	302	1.1	56.9	21.7 ± 1.4	28	31 ± 1
JICA-A03	112	2.5	3.5	6.8	8.4	6.9	360	4.6	10.1	21.4 ± 1.3	38	111 ± 3
JST- 001 (2)	10.2	2.3	3.4	6.9	9.1	22.4	420	8.9	1.1	20.3 ± 0.4	29	9.6 ± 0.1
JST -001 (1)	10.4	2.3	3.4	6.6	8.4	22.7	420	3.5	17.4	21.7 ± 1.4	30	9.8 ± 0.3
JICA-A01	163	2.3	3.1	6.1	8.1	5.9	574	4.2	12.1	25.2 ± 0.7	30	162 ± 2
B-06 (2)	31.5	2.3	3.4	7.0	9.1	0.4	650	7.5	2.4	20.4 ± 0.4	30	30.9 ± 0.5
B-07 (2)	28.5	2.3	3.4	7.1	9.2	0.5	575	6.1	4.7	19.8 ± 0.4	30	27.9 ± 0.4
B-07 (1)	28	2.4	3.4	7.0	9.0	0.5	575	1.8	41.3	20.1 ± 1.3	31	27.4 ± 0.8
JST-002 (2)	78.5	2.4	3.3	6.8	8.8	0.6	605	8.0	1.9	21.5 ± 0.4	33	78 ± 1
JST-002 (1)	78.7	2.4	3.4			0.7	605	-	-	-	-	-
Uncertainty (%)	1.3 - 3.5	0.9 - 2.4	1.3 - 3.3	2.5 - 8.1	4.5 - 9.1	0.2 - 7.8						

Table 6. ^{81}Kr and ^{85}Kr data for groundwaters from the lower Chao Phraya River basin. The ^{81}Kr and ^{14}C apparent ages calculated assuming piston flow conditions are reported. The concentrations of radiogenic ^{4}He are also shown for comparison.

Sample name	Aquifer	^{85}Kr (dpm/cc)	^{81}Kr (pMKr)	^{81}Kr age (ka)	^{81}Kr age[##] (ka)	^{14}C age (ka)	^{4}He radiogenic (10^{-7} cm^3STP/g)
JICA-A05	SK	3.62 ± 0.23	95 ± 3	17.0 ± 0.5	18.0 ± 0.5	26 ± 5	6.3 ± 0.2
PT0022		0.78 ± 0.16	95 ± 3	17.0 ± 0.5		12 ± 2	6.9 ± 0.2
JICA-A04	PT	0.40 ± 0.13	65 ± 3	142 ± 7		-	31 ± 1
JICA-A03	TB	0.68 ± 0.13	42 ± 2	287 ± 14		-	111 ± 3
JST-001		< 0.59	86 ± 3	50 ± 2		-	9.6 ± 0.1
B06	PN	< 0.57	85 ± 3	54 ± 2		13 ± 3	30.9 ± 0.5
B07[#]		31.4 ± 1.0	87 ± 3	46 ± 2	80 ± 3	-	27.9 ± 0.4
JST-002		0.61 ± 0.08	70 ± 3	118 ± 5		23 ± 5	78 ± 1

[#] Apparent sampling problem from the water reservoir open to air as evident from ^{85}Kr of > 30 dpm/cm^3 (Kr).
[##] Ages after correction for contamination with modern air.

Figure 1. (a) Map with the location of the sampling points in the study area, and (b) 3D map of the lower Chao Phraya River Basin, taken from Sanford and Buapeng [1].

Figure 2. Hydrogeological profile of the Bangkok aquifer system, with approximate location of the eight studied aquifers.

Figure 3. Relationships of various ion concentrations in groundwater from the investigated area: a) (Ca^{2+}+Mg^{2+}) vs. HCO_3^-; b) (Ca^{2+}+Mg^{2+}) vs. (HCO_3^-+SO_4^{2-}); c) ((Na^++K^+)-Cl^-) vs. ((Ca^{2+}+Mg^{2+})-(HCO_3-+SO_4^{2-})); and d) Na^+ vs. Cl^-. Samples are separated according to their depths, in shallow (dark triangles) and deep (inverse light grey triangles) aquifers.

Figure 4. a) $\delta^{18}O$ versus δ^2H in groundwater samples from the study area. Samples are separated according to their depths, in shallow (dark triangles) and deep (inverse light grey triangles) aquifers. The local and global meteoric water lines (LMWL and GMWL) are also shown. A line representing evaporation and/or mixing processes is also depicted. b) Variation of $\delta^{18}O$ in groundwater versus depth in m below ground level (bgl) in the study area. The mean $\delta^{18}O$ in Bangkok precipitation is also shown. Shallow wells tend to show enriched values compared to deep wells.

Figure 5. Variations of the ^{14}C, ^{81}Kr and ^4He concentrations with depth. Shaded areas contain wells that are located in the eastern or western part of the lower Chao Phraya River Basin.

Figure 6. Variation of the recharge temperature (NGT) and the excess air component (expressed as %ΔNe) with the well depth in the study area. Samples are separated according to their depths, in shallow (dark triangles) and deep (inverse light grey triangles) aquifers. Shallow wells tend to show lower %ΔNe and higher NGT than deep wells.

Figure 7. $^3He/^4He$ ratio vs. Ne/He ratio in groundwater from the study area. Samples are separated according to their depths, in shallow (dark triangles) and deep (inverse light grey triangles) aquifers. The mean ratios corresponding to crustal, mantle and atmospheric sources are shown (represented with black circles). Mixing between different sources are represented by lines. The addition of 5%, 10% and 20% mantle

helium to hypothetical samples containing a mixture of air and crustal helium is represented with discontinuous lines.

Figure 8. Relationship of the concentrations of radiogenic ^{4}He with: a) ^{14}C apparent ages and b) the ^{81}Kr apparent ages. Samples are separated according to their depths, in shallow (dark triangles) and deep (inverse light grey triangles) aquifers. Also, the relationships of the ^{4}He model ages with: a) the ^{14}C apparent ages, and b) the ^{81}Kr ages are shown

Figure 9. Comparison of tracer ages obtained from ^{14}C, ^{81}Kr and ^{4}He data

FIGURES

Figure 1

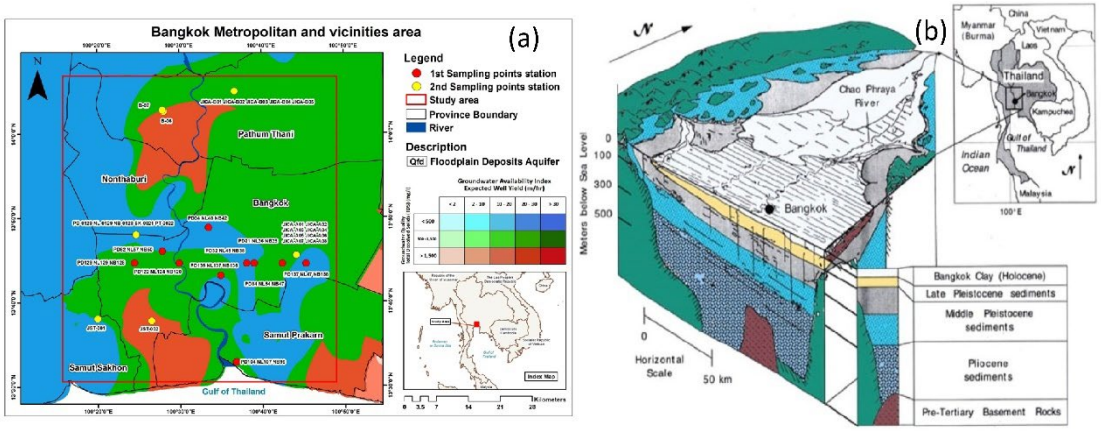

Figure 2

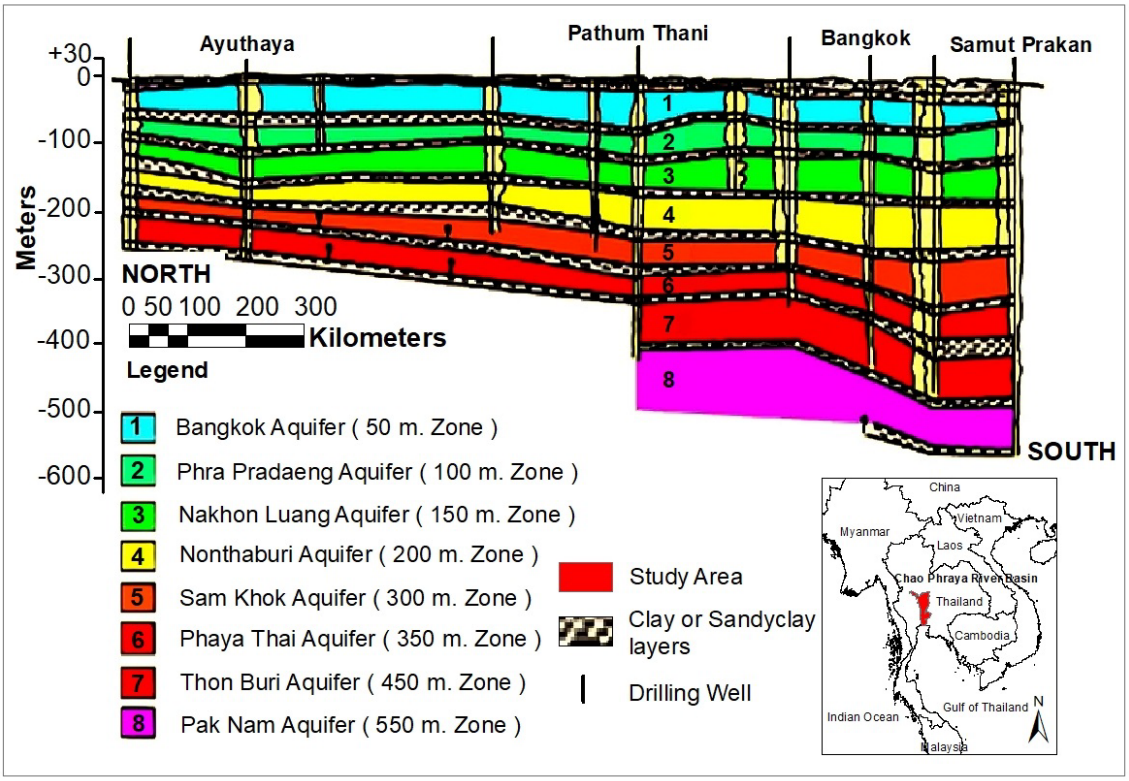

Figure 3

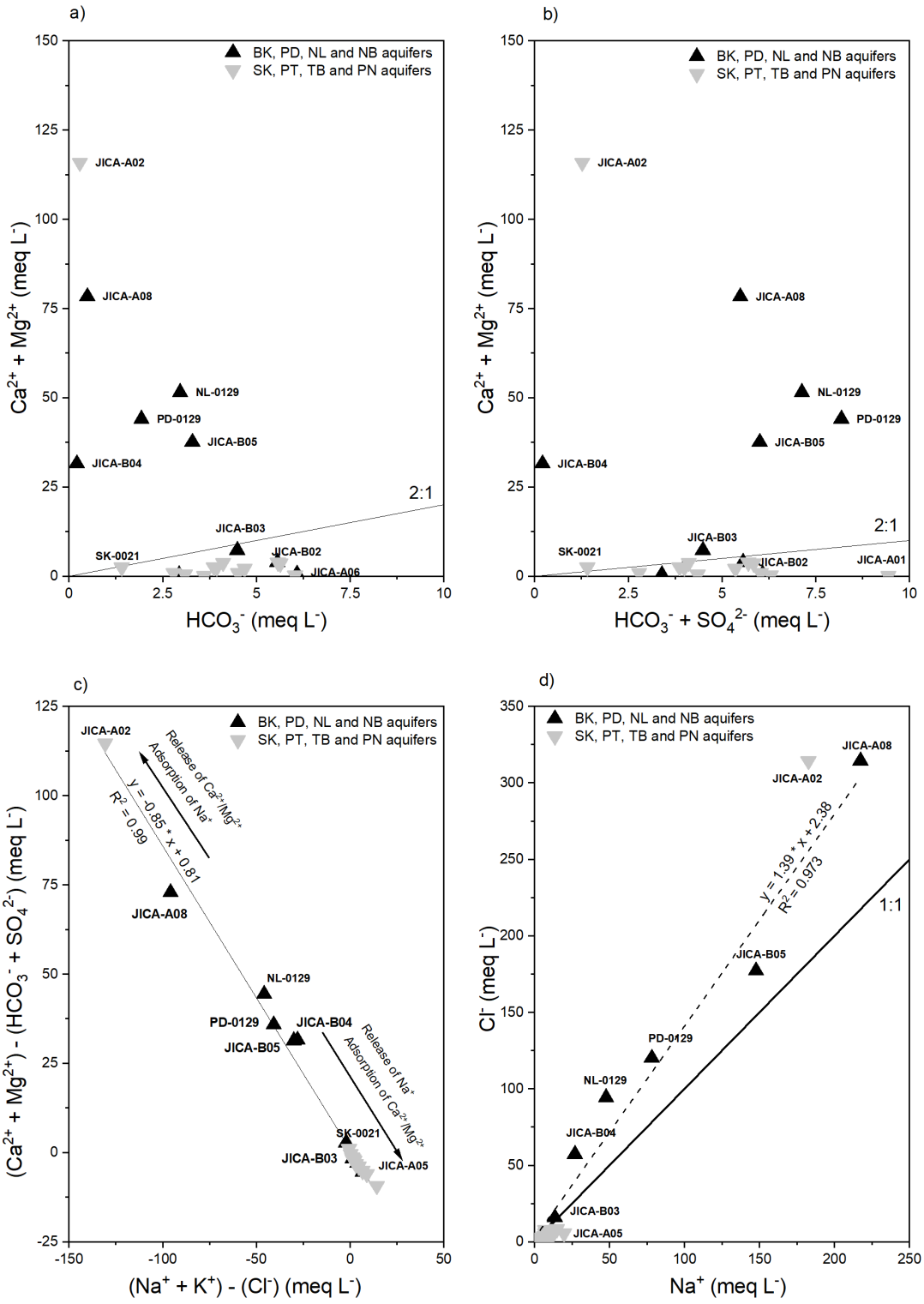

Figure 4

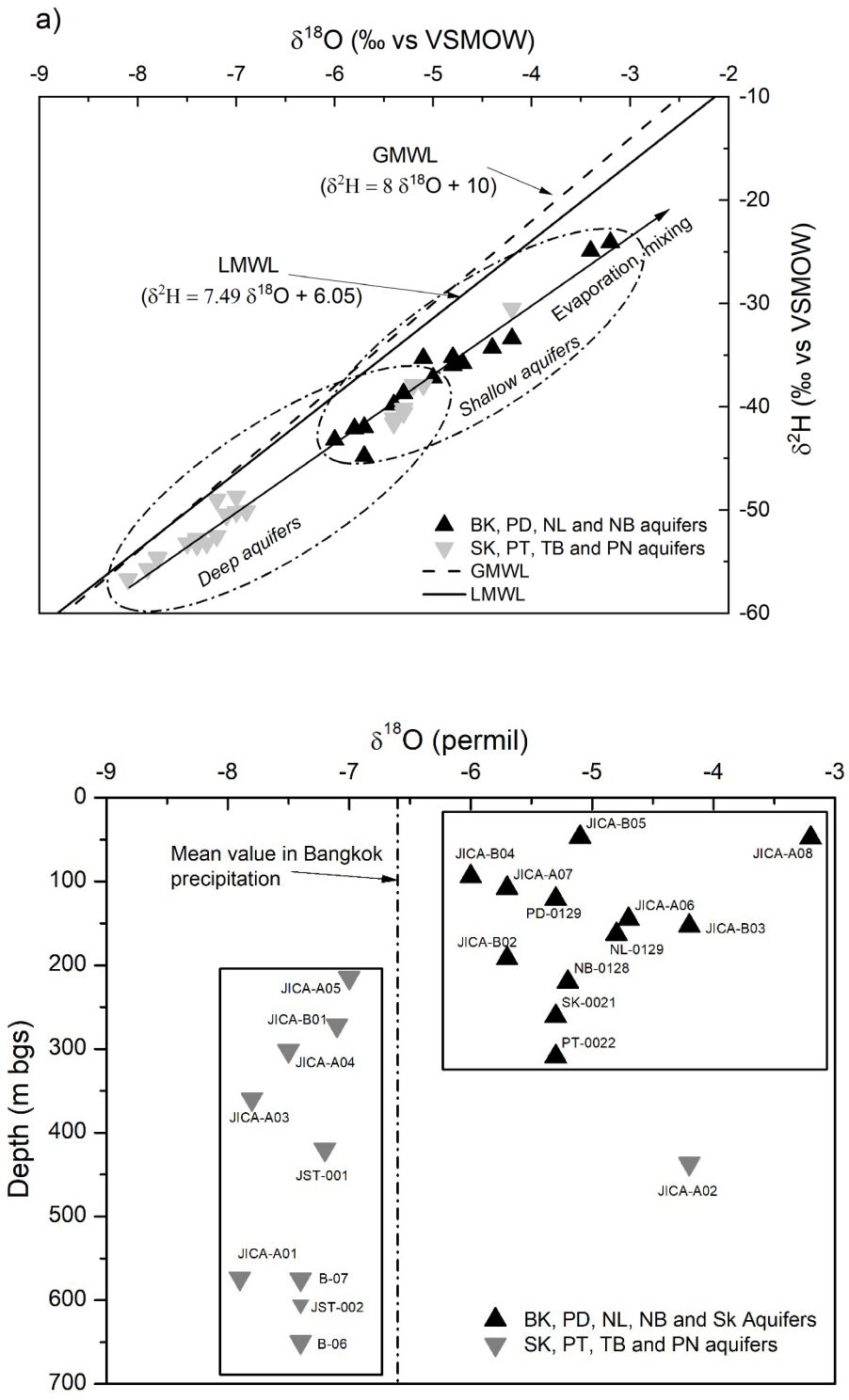
a)
δ18O (‰ vs VSMOW)
δ2H (‰ vs VSMOW)
GMWL
(δ2H = 8 δ18O + 10)
LMWL
(δ2H = 7.49 δ18O + 6.05)
Evaporation / mixing
Shallow aquifers
Deep aquifers
BK, PD, NL and NB aquifers
SK, PT, TB and PN aquifers
GMWL
LMWL
δ18O (permil)
Depth (m bgs)
Mean value in Bangkok precipitation
JICA-B05
JICA-B04
JICA-A08
JICA-A07
PD-0129
JICA-A06
JICA-B03
JICA-B02
NL-0129
NB-0128
SK-0021
PT-0022
JICA-A05
JICA-B01
JICA-A04
JICA-A03
JST-001
JICA-A02
JICA-A01
B-07
JST-002
B-06
BK, PD, NL, NB and Sk Aquifers
SK, PT, TB and PN aquifers

Figure 5

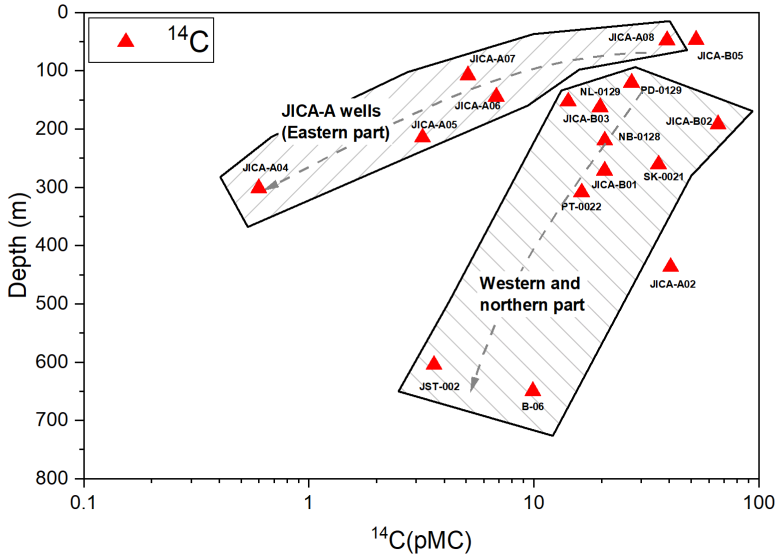
^{14}C
JICA-A08
JICA-B05
JICA-A07
JICA-A06
JICA-A05
JICA-A04
JICA-A wells
(Eastern part)
NL-0129
PD-0129
JICA-B03
JICA-B02
NB-0128
SK-0021
JICA-B01
PT-0022
JICA-A02
Western and
northern part
JST-002
B-06
Depth (m)
0
100
200
300
400
500
600
700
800
0.1
1
10
100
^{14}C(pMC)

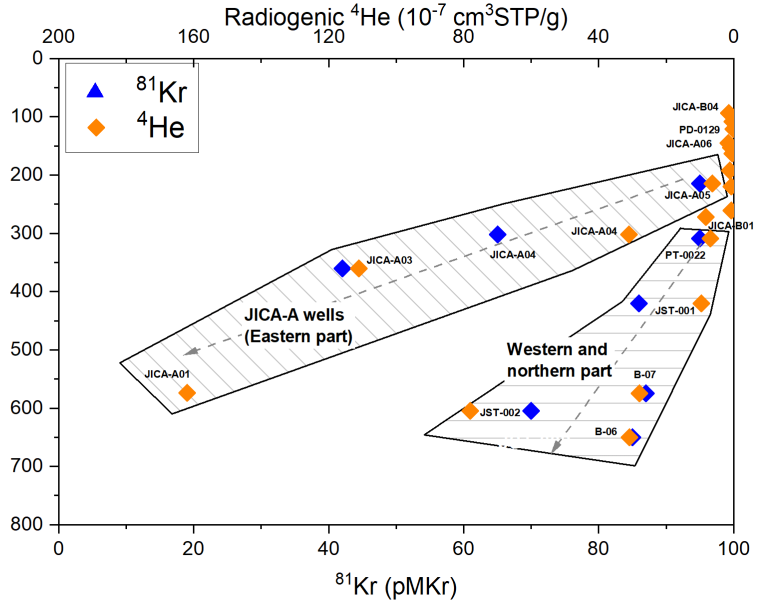
Radiogenic ^{4}He (10^{-7} cm^{3}STP/g)
200
160
120
80
40
0
^{81}Kr
^{4}He
JICA-B04
PD-0129
JICA-A06
JICA-A05
JICA-B01
JICA-A04
JICA-A03
JICA-A04
PT-0022
JST-001
JICA-A wells
(Eastern part)
Western and
northern part
JICA-A01
B-07
JST-002
B-06
0
100
200
300
400
500
600
700
800
0
20
40
60
80
100
^{81}Kr (pMKr)

Figure 6

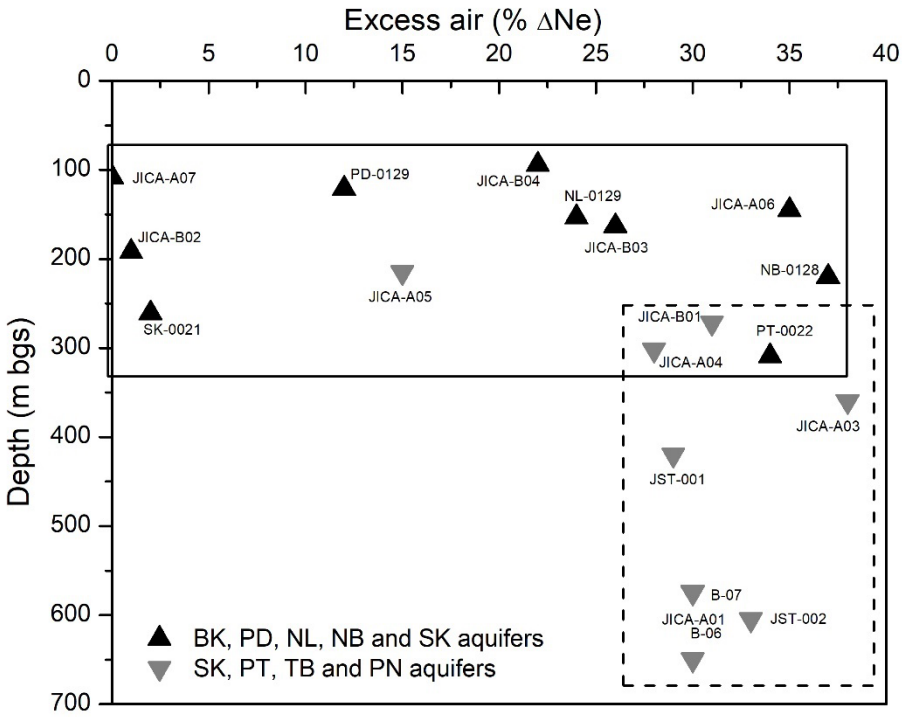

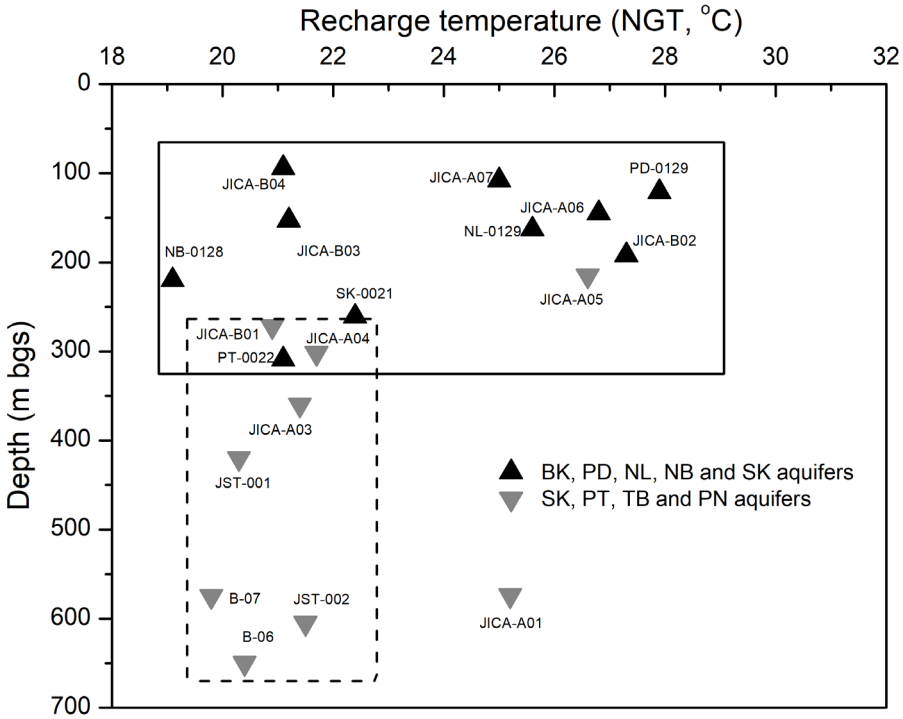

Figure 7

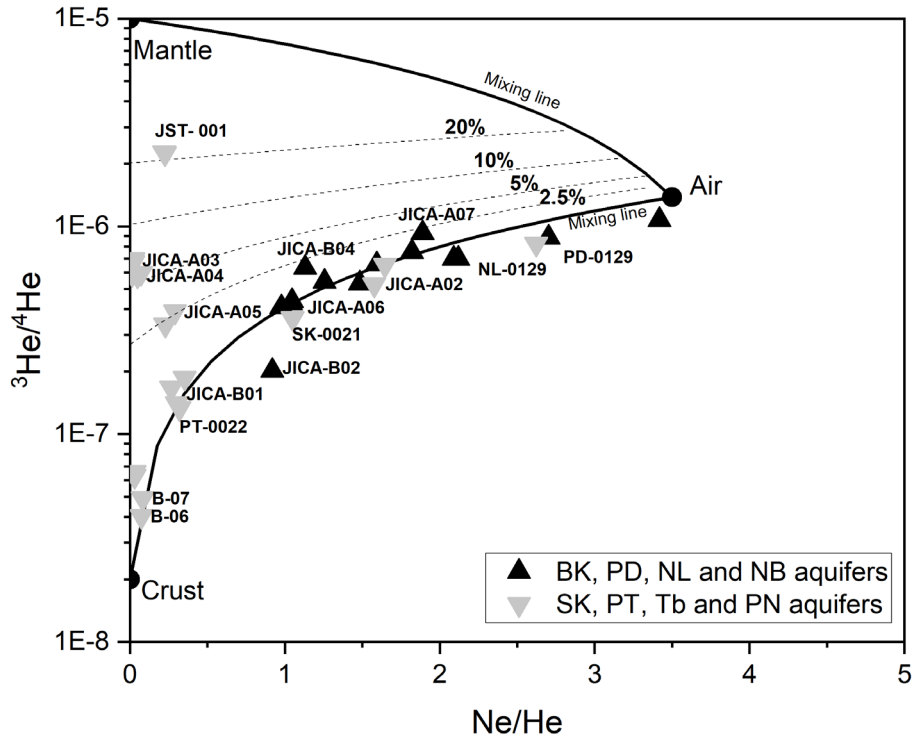

Figure 8

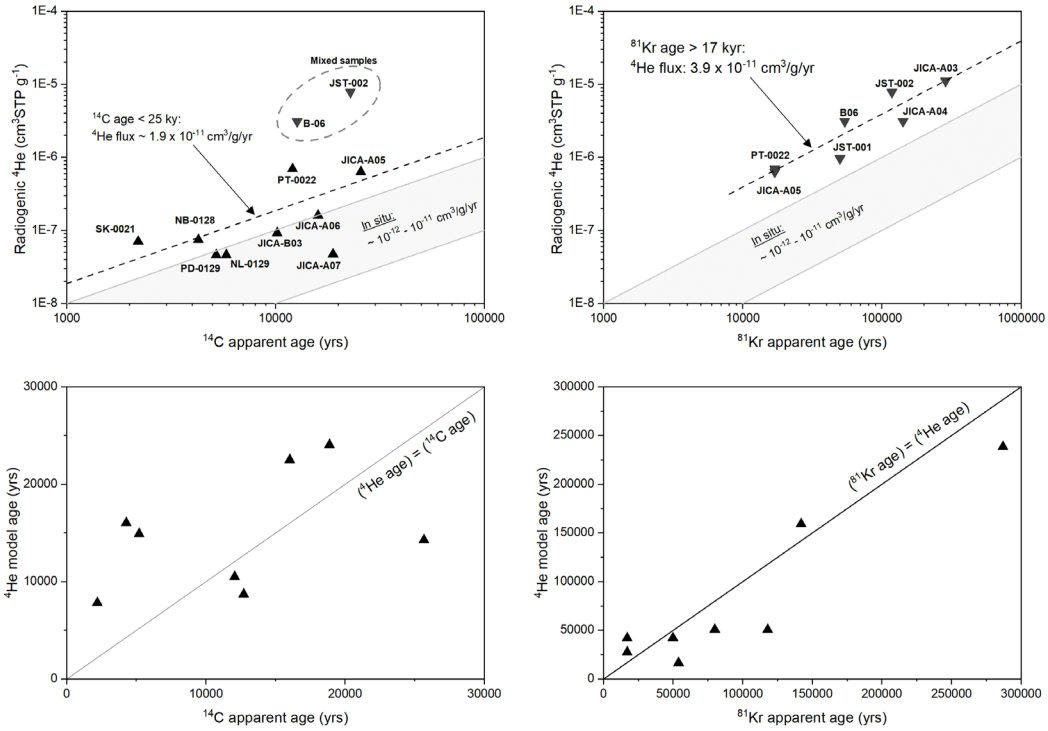

Figure 9

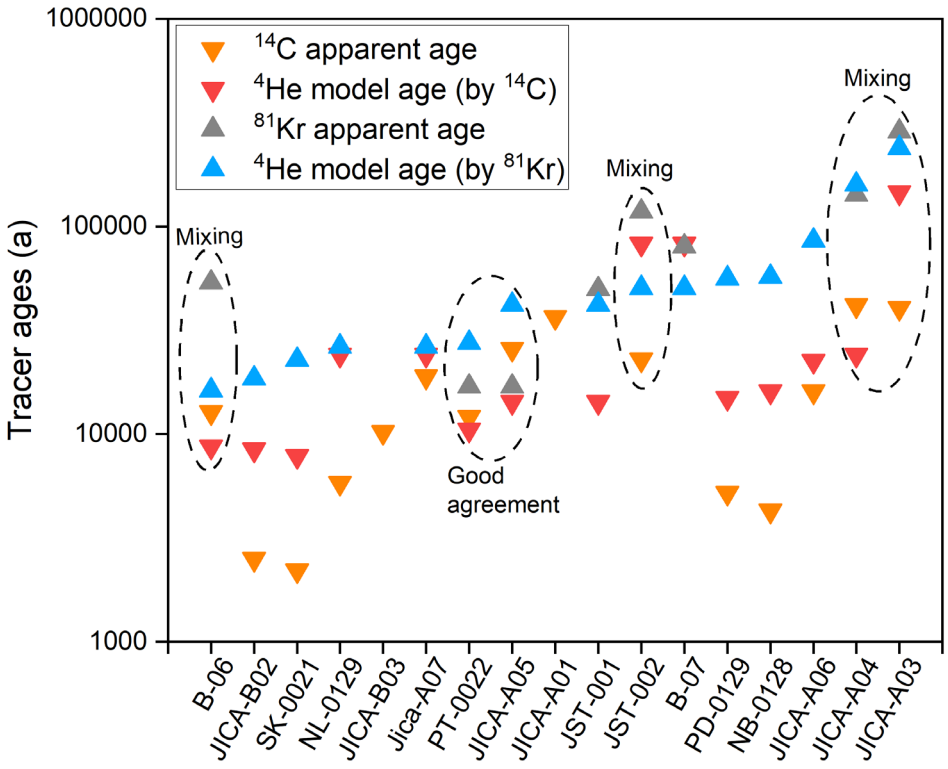
1000000
100000
10000
1000
Tracer ages (a)
^{14}C apparent age
^{4}He model age (by ^{14}C)
^{81}Kr apparent age
^{4}He model age (by ^{81}Kr)
Mixing
Good agreement
Mixing
Mixing
B-06
JICA-B02
SK-0021
NL-0129
JICA-B03
Jica-A07
PT-0022
JICA-A05
JICA-A01
JST-001
JST-002
B-07
PD-0129
NB-0128
JICA-A06
JICA-A04
JICA-A03